

Analyse de données non stationnaires : représentations, théorie, algorithmes et applications.

Barbara Pascal

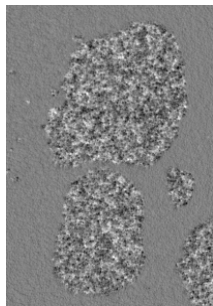
March 7th 2022

Laboratoire Mathématiques Appliquées À Paris 5 (MAP5)

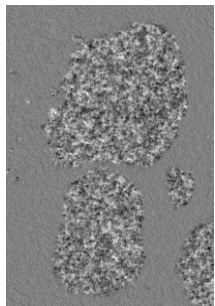
Groupe de travail Images

Part I: Texture segmentation based on fractal attributes

Textured image segmentation



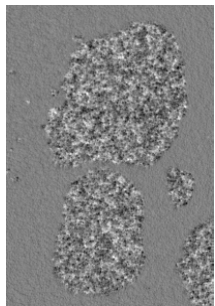
Textured image segmentation



Goal: obtain a partition of the image into K homogeneous textures

$$\Omega = \Omega_1 \sqcup \dots \sqcup \Omega_K$$

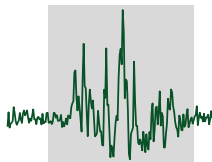
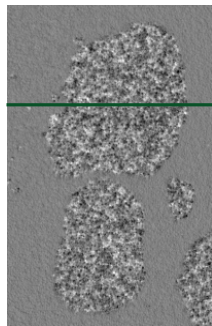
Textured image segmentation



Goal: obtain a partition of the image into K **homogeneous textures**

$$\Omega = \Omega_1 \sqcup \dots \sqcup \Omega_K$$

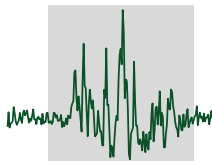
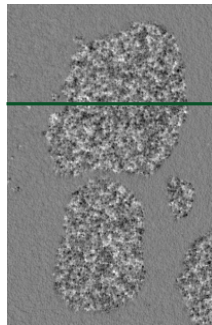
Piecewise monofractal model



Piecewise monofractal model

Fractals attributes

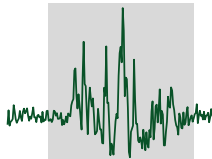
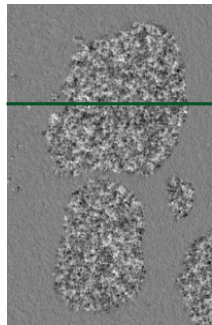
- variance σ^2 *amplitude of variations*



Piecewise monofractal model

Fractals attributes

- variance σ^2 *amplitude of variations*
- local regularity h *scale invariance*

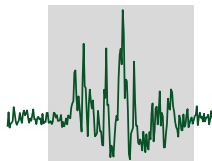
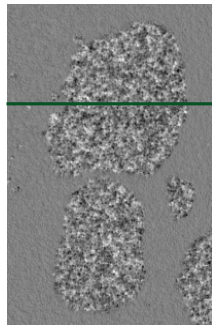


Piecewise monofractal model

Fractals attributes

- variance σ^2 *amplitude of variations*
- local regularity h *scale invariance*

$$|f(x) - f(y)| \leq \sigma(x)|x - y|^{h(x)}$$



Piecewise monofractal model

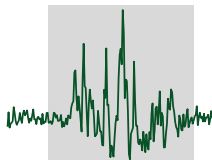
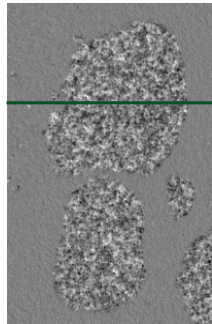
Fractals attributes

- variance σ^2 *amplitude of variations*
- local regularity h *scale invariance*

$$|f(x) - f(y)| \leq \sigma(x)|x - y|^{h(x)}$$



$$h(x) \equiv h_1 = 0.9 \quad h(x) \equiv h_2 = 0.3$$



Piecewise monofractal model

Fractals attributes

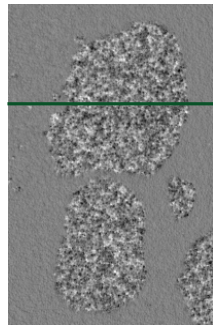
- variance σ^2 *amplitude of variations*
- local regularity h *scale invariance*

$$|f(x) - f(y)| \leq \sigma(x)|x - y|^{h(x)}$$



$$h(x) \equiv h_1 = 0.9$$

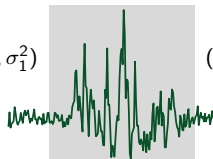
$$h(x) \equiv h_2 = 0.3$$



$$(h_2, \sigma_2^2)$$

$$(h_1, \sigma_1^2)$$

$$(h_1, \sigma_1^2)$$



Segmentation

- σ^2 and h piecewise constant

Piecewise monofractal model

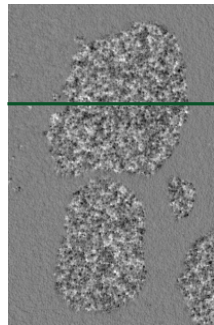
Fractals attributes

- variance σ^2 *amplitude of variations*
- local regularity h *scale invariance*

$$|f(x) - f(y)| \leq \sigma(x)|x - y|^{h(x)}$$

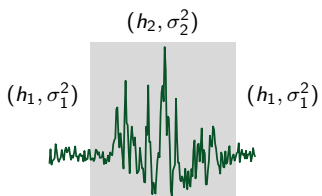


$$h(x) \equiv h_1 = 0.9 \quad h(x) \equiv h_2 = 0.3$$



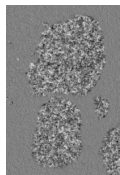
Segmentation

- ▶ σ^2 and h piecewise constant
- ▶ region Ω_k characterized by (σ_k^2, h_k)



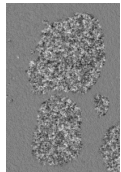
Multiscale analysis

Textured image



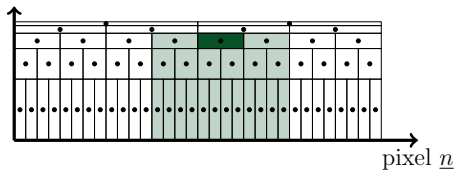
Multiscale analysis

Textured image



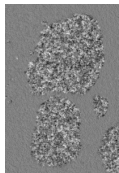
Local maximum of wavelet coefficients: $\mathcal{L}_{a,\cdot}$

scale 2^j



Multiscale analysis

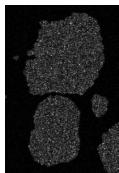
Textured image



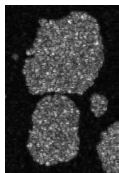
Local maximum of wavelet coefficients: $\mathcal{L}_{a,\cdot}$

Scale

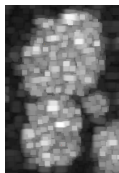
$a = 2^1$



$a = 2^2$

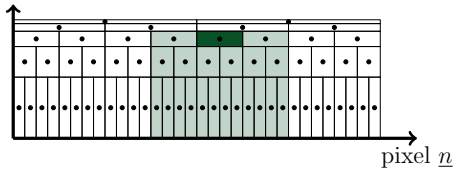


$a = 2^5$



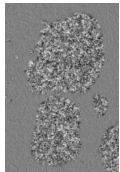
...

scale 2^j



Multiscale analysis

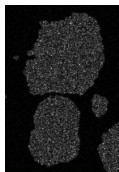
Textured image



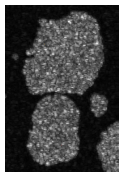
Local maximum of wavelet coefficients: $\mathcal{L}_{a,\cdot}$

Scale

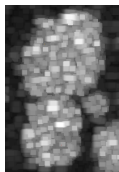
$a = 2^1$



$a = 2^2$



$a = 2^5$



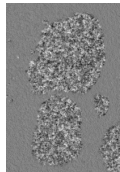
...

Proposition (Jaffard, 2004), (Wendt, 2008)

$$\log(\mathcal{L}_{a,\cdot}) \underset{a \rightarrow 0}{\simeq} \log(a) \underset{\text{regularity}}{h} + \underset{\propto \log(\sigma^2)}{\nu} \underset{\text{(variance)}}{}$$

Multiscale analysis

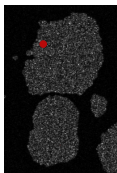
Textured image



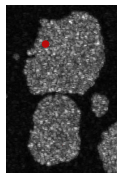
Local maximum of wavelet coefficients: $\mathcal{L}_{a,\cdot}$

Scale

$a = 2^1$

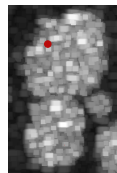


$a = 2^2$



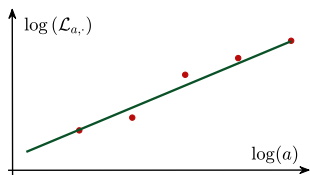
...

$a = 2^5$



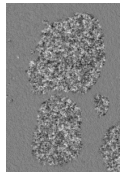
Proposition (Jaffard, 2004), (Wendt, 2008)

$$\log(\mathcal{L}_{a,\cdot}) \underset{a \rightarrow 0}{\simeq} \log(a) \begin{matrix} h \\ \text{regularity} \end{matrix} + \begin{matrix} v \\ \propto \log(\sigma^2) \\ (\text{variance}) \end{matrix}$$



Multiscale analysis

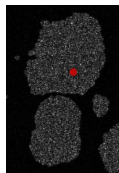
Textured image



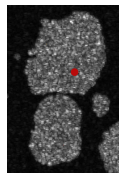
Local maximum of wavelet coefficients: $\mathcal{L}_{a,\cdot}$

Scale

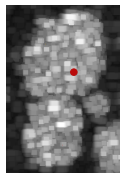
$a = 2^1$



$a = 2^2$



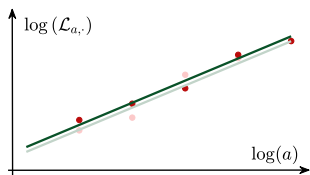
$a = 2^5$



...

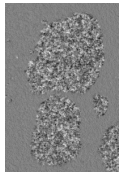
Proposition (Jaffard, 2004), (Wendt, 2008)

$$\log(\mathcal{L}_{a,\cdot}) \underset{a \rightarrow 0}{\simeq} \log(a) \begin{matrix} h \\ \text{regularity} \end{matrix} + \begin{matrix} v \\ \propto \log(\sigma^2) \\ (\text{variance}) \end{matrix}$$



Multiscale analysis

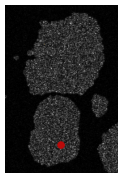
Textured image



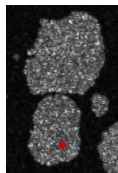
Local maximum of wavelet coefficients: $\mathcal{L}_{a,\cdot}$

Scale

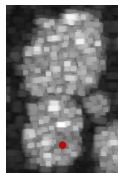
$a = 2^1$



$a = 2^2$



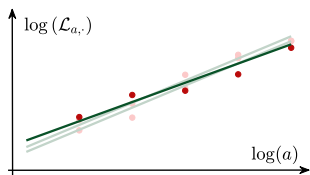
$a = 2^5$



...

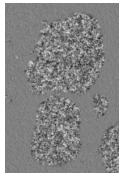
Proposition (Jaffard, 2004), (Wendt, 2008)

$$\log(\mathcal{L}_{a,\cdot}) \underset{a \rightarrow 0}{\simeq} \log(a) \begin{matrix} h \\ \text{regularity} \end{matrix} + \begin{matrix} v \\ \propto \log(\sigma^2) \\ (\text{variance}) \end{matrix}$$



Multiscale analysis

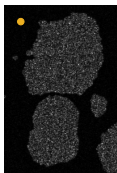
Textured image



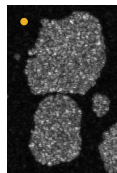
Local maximum of wavelet coefficients: $\mathcal{L}_{a,\cdot}$

Scale

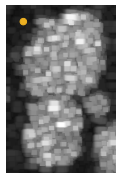
$a = 2^1$



$a = 2^2$



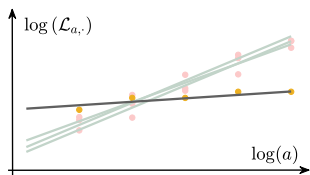
$a = 2^5$



...

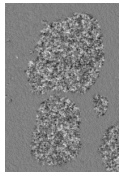
Proposition (Jaffard, 2004), (Wendt, 2008)

$$\log(\mathcal{L}_{a,\cdot}) \underset{a \rightarrow 0}{\simeq} \log(a) \begin{matrix} h \\ \text{regularity} \end{matrix} + \begin{matrix} v \\ \propto \log(\sigma^2) \\ (\text{variance}) \end{matrix}$$



Multiscale analysis

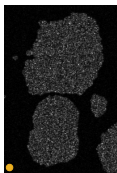
Textured image



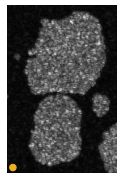
Local maximum of wavelet coefficients: $\mathcal{L}_{a,\cdot}$

Scale

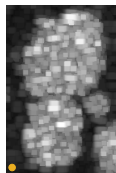
$a = 2^1$



$a = 2^2$



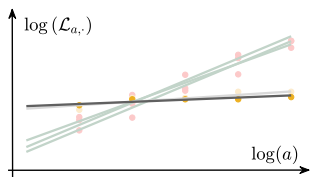
$a = 2^5$



...

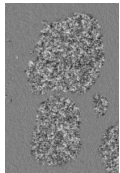
Proposition (Jaffard, 2004), (Wendt, 2008)

$$\log(\mathcal{L}_{a,\cdot}) \underset{a \rightarrow 0}{\simeq} \log(a) \begin{matrix} h \\ \text{regularity} \end{matrix} + \begin{matrix} v \\ \propto \log(\sigma^2) \\ (\text{variance}) \end{matrix}$$



Multiscale analysis

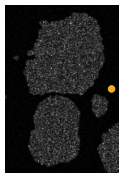
Textured image



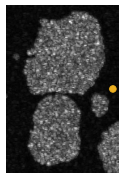
Local maximum of wavelet coefficients: $\mathcal{L}_{a,\cdot}$

Scale

$a = 2^1$

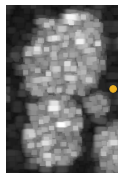


$a = 2^2$



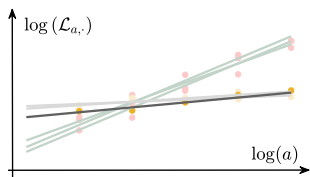
...

$a = 2^5$



Proposition (Jaffard, 2004), (Wendt, 2008)

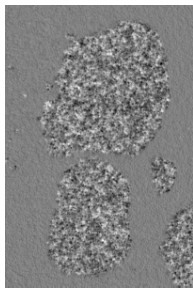
$$\log(\mathcal{L}_{a,\cdot}) \underset{a \rightarrow 0}{\simeq} \log(a) \underset{\text{regularity}}{h} + \underset{\propto \log(\sigma^2)}{\nu} \underset{\text{(variance)}}{}$$



Direct punctual estimation

Linear regression $\log(\mathcal{L}_{a,\cdot}) \simeq \log(a) \frac{\boldsymbol{h}}{\text{regularity}} + \frac{\boldsymbol{v}}{\propto \log(\sigma^2)}$

Textured image

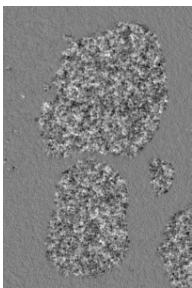


Direct punctual estimation

Linear regression $\log(\mathcal{L}_{a,\cdot}) \simeq \log(a) \frac{\boldsymbol{h}}{\text{regularity}} + \frac{\boldsymbol{v}}{\propto \log(\sigma^2)}$

$$(\hat{\boldsymbol{h}}^{\text{LR}}, \hat{\boldsymbol{v}}^{\text{LR}}) = \underset{\boldsymbol{h}, \boldsymbol{v}}{\text{argmin}} \sum_{a=a_{\min}}^{a_{\max}} \|\log(\mathcal{L}_{a,\cdot}) - \log(a)\boldsymbol{h} - \boldsymbol{v}\|^2$$

Textured image

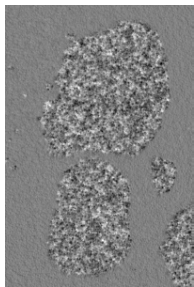


Direct punctual estimation

Linear regression $\log(\mathcal{L}_{a,\cdot}) \simeq \log(a) \frac{\boldsymbol{h}}{\text{regularity}} + \frac{\boldsymbol{v}}{\propto \log(\sigma^2)}$

$$(\hat{\boldsymbol{h}}^{\text{LR}}, \hat{\boldsymbol{v}}^{\text{LR}}) = \underset{\boldsymbol{h}, \boldsymbol{v}}{\operatorname{argmin}} \sum_{a=a_{\min}}^{a_{\max}} \|\log(\mathcal{L}_{a,\cdot}) - \log(a)\boldsymbol{h} - \boldsymbol{v}\|^2$$

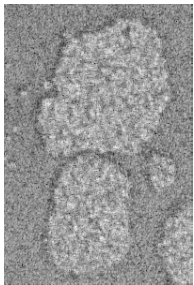
Textured image



Local regularity $\hat{\boldsymbol{h}}^{\text{LR}}$



Local power $\hat{\boldsymbol{v}}^{\text{LR}}$

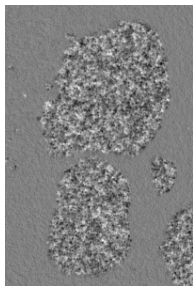


Direct punctual estimation

Linear regression $\mathbb{E} \log(\mathcal{L}_{a,\cdot}) = \log(a) \underset{\text{regularity}}{\bar{h}} + \underset{\propto \log(\sigma^2)}{\bar{v}}$

$$(\hat{\mathbf{h}}^{\text{LR}}, \hat{\mathbf{v}}^{\text{LR}}) = \operatorname{argmin}_{\mathbf{h}, \mathbf{v}} \sum_{a=a_{\min}}^{a_{\max}} \|\log(\mathcal{L}_{a,\cdot}) - \log(a)\mathbf{h} - \mathbf{v}\|^2$$

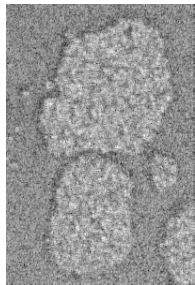
Textured image



Local regularity $\hat{\mathbf{h}}^{\text{LR}}$



Local power $\hat{\mathbf{v}}^{\text{LR}}$



→ large estimation variance

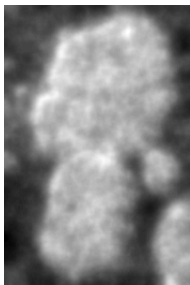
Filter smoothing (linear)

$$\left(\mathbf{I} + \lambda \mathbf{D}^\top \mathbf{D}\right)^{-1} \hat{\mathbf{h}}^{\text{LR}}$$

Linear regression $\hat{\mathbf{h}}^{\text{LR}}$



Lissage



A posteriori regularization

Filter smoothing (linear)

$$\left(\mathbf{I} + \lambda \mathbf{D}^\top \mathbf{D}\right)^{-1} \hat{\mathbf{h}}^{\text{LR}}$$

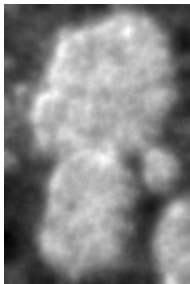
Linear regression $\hat{\mathbf{h}}^{\text{LR}}$



ROF denoising (nonlinear)

$$\operatorname{argmin}_{\mathbf{h}} \|\mathbf{h} - \hat{\mathbf{h}}^{\text{LR}}\|^2 + \lambda \|\mathbf{D}\mathbf{h}\|_{2,1}$$

Lissage



ROF

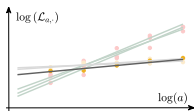


→ cumulative estimation variance and regularization bias

Functionals with either free or co-localized contours

$$\sum_a \frac{\|\log \mathcal{L}_{a,.} - \log(a) \mathbf{h} - \mathbf{v}\|^2}{\text{Least-Squares}}$$

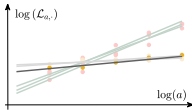
→ fidelity to the log-linear model



Functionals with either free or co-localized contours

$$\sum_a \frac{\|\log \mathcal{L}_{a,.} - \log(a) \mathbf{h} - \mathbf{v}\|^2}{\text{Least-Squares}} + \lambda \frac{\mathcal{Q}(\mathbf{D}\mathbf{h}, \mathbf{D}\mathbf{v}; \alpha)}{\text{Total Variation}}$$

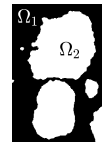
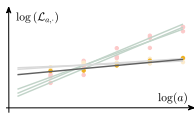
\rightarrow fidelity to the log-linear model
 \rightarrow favors piecewise constancy



Functionals with either free or co-localized contours

$$\underset{\mathbf{h}, \mathbf{v}}{\text{minimize}} \quad \sum_a \frac{\|\log \mathcal{L}_{a,.} - \log(a) \mathbf{h} - \mathbf{v}\|^2}{\text{Least-Squares}} + \lambda \frac{\mathcal{Q}(\mathbf{D}\mathbf{h}, \mathbf{D}\mathbf{v}; \alpha)}{\text{Total Variation}}$$

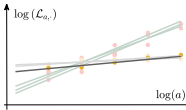
\rightarrow fidelity to the log-linear model
 \rightarrow favors piecewise constancy



Functionals with either free or co-localized contours

$$\underset{\mathbf{h}, \mathbf{v}}{\text{minimize}} \quad \sum_a \frac{\|\log \mathcal{L}_{a,.} - \log(a) \mathbf{h} - \mathbf{v}\|^2}{\text{Least-Squares}} + \lambda \frac{\mathcal{Q}(\mathbf{D}\mathbf{h}, \mathbf{D}\mathbf{v}; \alpha)}{\text{Total Variation}}$$

\rightarrow fidelity to the log-linear model
 \rightarrow favors piecewise constancy

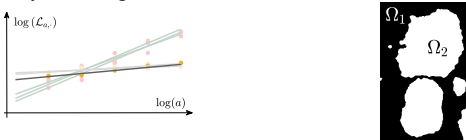


Finite differences $\mathbf{D}_1 \mathbf{x}$ (horizontal), $\mathbf{D}_2 \mathbf{x}$ (vertical) in each pixel

Functionals with either free or co-localized contours

$$\underset{\mathbf{h}, \mathbf{v}}{\text{minimize}} \quad \sum_a \frac{\|\log \mathcal{L}_{a,.} - \log(a)\mathbf{h} - \mathbf{v}\|^2}{\text{Least-Squares}} + \lambda \frac{\mathcal{Q}(\mathbf{D}\mathbf{h}, \mathbf{D}\mathbf{v}; \alpha)}{\text{Total Variation}}$$

\rightarrow fidelity to the log-linear model
 \rightarrow favors piecewise constancy



Finite differences $\mathbf{D}\mathbf{x} = [\mathbf{D}_1\mathbf{x}, \mathbf{D}_2\mathbf{x}]$

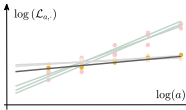
Free: \mathbf{h} , \mathbf{v} are **independently** piecewise constant

$$\mathcal{Q}_F(\mathbf{D}\mathbf{h}, \mathbf{D}\mathbf{v}; \alpha) = \alpha \|\mathbf{D}\mathbf{h}\|_{2,1} + \|\mathbf{D}\mathbf{v}\|_{2,1}$$

Functionals with either free or co-localized contours

$$\underset{\mathbf{h}, \mathbf{v}}{\text{minimize}} \quad \sum_a \frac{\|\log \mathcal{L}_{a,.} - \log(a)\mathbf{h} - \mathbf{v}\|^2}{\text{Least-Squares}} + \lambda \frac{\mathcal{Q}(\mathbf{D}\mathbf{h}, \mathbf{D}\mathbf{v}; \alpha)}{\text{Total Variation}}$$

\rightarrow fidelity to the log-linear model
 \rightarrow favors piecewise constancy



Finite differences $\mathbf{D}\mathbf{x} = [\mathbf{D}_1\mathbf{x}, \mathbf{D}_2\mathbf{x}]$

Free: \mathbf{h} , \mathbf{v} are **independently** piecewise constant

$$\mathcal{Q}_F(\mathbf{D}\mathbf{h}, \mathbf{D}\mathbf{v}; \alpha) = \alpha \|\mathbf{D}\mathbf{h}\|_{2,1} + \|\mathbf{D}\mathbf{v}\|_{2,1}$$

Co-localized: \mathbf{h} , \mathbf{v} are **concomitantly** piecewise constant

$$\mathcal{Q}_C(\mathbf{D}\mathbf{h}, \mathbf{D}\mathbf{v}; \alpha) = \|[\alpha \mathbf{D}\mathbf{h}, \mathbf{D}\mathbf{v}]\|_{2,1}$$

Functionals minimization

$$\underset{\mathbf{h}, \mathbf{v}}{\text{minimize}} \quad \sum_a \frac{\|\log \mathcal{L}_{a,.} - \log(a)\mathbf{h} - \mathbf{v}\|^2}{\text{Least-Squares}} + \lambda \frac{\mathcal{Q}(\mathbf{D}\mathbf{h}, \mathbf{D}\mathbf{v}; \alpha)}{\text{Total Variation}}$$



Functionals minimization

$$\underset{\mathbf{h}, \mathbf{v}}{\text{minimize}} \quad \sum_a \frac{\|\log \mathcal{L}_{a,.} - \log(a) \mathbf{h} - \mathbf{v}\|^2}{\text{Least-Squares}} + \lambda \frac{\mathcal{Q}(\mathbf{D}\mathbf{h}, \mathbf{D}\mathbf{v}; \alpha)}{\text{Total Variation}}$$



- gradient descent $\mathbf{x}^{n+1} = \mathbf{x}^n - \tau \nabla \varphi(\mathbf{x}^n)$

Functionals minimization

$$\underset{\mathbf{h}, \mathbf{v}}{\text{minimize}} \quad \sum_a \frac{\|\log \mathcal{L}_{a,.} - \log(a) \mathbf{h} - \mathbf{v}\|^2}{\text{Least-Squares}} + \lambda \frac{\mathcal{Q}(\mathbf{D}\mathbf{h}, \mathbf{D}\mathbf{v}; \alpha)}{\text{Total Variation}}$$



nonsmooth



- ▶ gradient descent $\mathbf{x}^{n+1} = \mathbf{x}^n - \tau \nabla \varphi(\mathbf{x}^n)$
- ▶ implicit subgradient descent: proximal point algorithm
$$\mathbf{x}^{n+1} = \mathbf{x}^n - \tau \mathbf{u}^n, \quad \mathbf{u}^n \in \partial \varphi(\mathbf{x}^{n+1}) \Leftrightarrow \mathbf{x}^{n+1} = \text{prox}_{\tau \varphi}(\mathbf{x}^n)$$

Functionals minimization

$$\underset{\mathbf{h}, \mathbf{v}}{\text{minimize}} \quad \sum_a \frac{\|\log \mathcal{L}_{a,.} - \log(a)\mathbf{h} - \mathbf{v}\|^2}{\text{Least-Squares}} + \lambda \frac{\mathcal{Q}(\mathbf{D}\mathbf{h}, \mathbf{D}\mathbf{v}; \alpha)}{\text{Total Variation}}$$



nonsmooth



- ▶ gradient descent $\mathbf{x}^{n+1} = \mathbf{x}^n - \tau \nabla \varphi(\mathbf{x}^n)$
- ▶ implicit subgradient descent: proximal point algorithm
$$\mathbf{x}^{n+1} = \mathbf{x}^n - \tau \mathbf{u}^n, \quad \mathbf{u}^n \in \partial \varphi(\mathbf{x}^{n+1}) \Leftrightarrow \mathbf{x}^{n+1} = \text{prox}_{\tau \varphi}(\mathbf{x}^n)$$
- ▶ splitting proximal algorithm

$$\mathbf{y}^{n+1} = \text{prox}_{\sigma(\lambda \mathcal{Q})^*} (\mathbf{y}^n + \sigma \mathbf{D} \bar{\mathbf{x}}^n)$$

$$\mathbf{x}^{n+1} = \text{prox}_{\tau \|\mathcal{L} - \Phi\cdot\|_2^2} \left(\mathbf{x}^n - \tau \mathbf{D}^\top \mathbf{y}^{n+1} \right), \quad \Phi : (\mathbf{h}, \mathbf{v}) \mapsto \{\log(a)\mathbf{h} + \mathbf{v}\}_a$$

$$\bar{\mathbf{x}}^{n+1} = 2\mathbf{x}^{n+1} - \mathbf{x}^n$$

Functionals minimization

$$\underset{\mathbf{h}, \mathbf{v}}{\text{minimize}} \quad \sum_a \frac{\|\log \mathcal{L}_{a,.} - \log(a)\mathbf{h} - \mathbf{v}\|^2}{\text{Least-Squares}} + \lambda \frac{\mathcal{Q}(\mathbf{D}\mathbf{h}, \mathbf{D}\mathbf{v}; \alpha)}{\text{Total Variation}}$$



nonsmooth



- ▶ gradient descent $\mathbf{x}^{n+1} = \mathbf{x}^n - \tau \nabla \varphi(\mathbf{x}^n)$
- ▶ implicit subgradient descent: proximal point algorithm
$$\mathbf{x}^{n+1} = \mathbf{x}^n - \tau \mathbf{u}^n, \quad \mathbf{u}^n \in \partial \varphi(\mathbf{x}^{n+1}) \Leftrightarrow \mathbf{x}^{n+1} = \text{prox}_{\tau \varphi}(\mathbf{x}^n)$$
- ▶ splitting proximal algorithm

$$\mathbf{y}^{n+1} = \text{prox}_{\sigma(\lambda \mathcal{Q})^*} (\mathbf{y}^n + \sigma \mathbf{D}\bar{\mathbf{x}}^n)$$

$$\mathbf{x}^{n+1} = \text{prox}_{\tau \|\mathcal{L} - \Phi\cdot\|_2^2} \left(\mathbf{x}^n - \tau \mathbf{D}^\top \mathbf{y}^{n+1} \right), \quad \Phi : (\mathbf{h}, \mathbf{v}) \mapsto \{\log(a)\mathbf{h} + \mathbf{v}\}_a$$

$$\bar{\mathbf{x}}^{n+1} = 2\mathbf{x}^{n+1} - \mathbf{x}^n$$

Accelerated algorithm based on strong-convexity

$$\underset{\mathbf{h}, \mathbf{v}}{\text{minimize}} \quad \sum_a \frac{\|\log \mathcal{L}_{a,.} - \log(a)\mathbf{h} - \mathbf{v}\|^2}{\text{Least-Squares}} + \lambda \frac{\mathcal{Q}(\mathbf{D}\mathbf{h}, \mathbf{D}\mathbf{v}; \alpha)}{\text{Total Variation}}$$



nonsmooth



Primal-dual algorithm (Chambolle, 2011)

$$\delta: \text{duality gap}, \delta(\mathbf{x}^n, \mathbf{y}^n) \xrightarrow{n \rightarrow \infty} 0$$

Accelerated algorithm based on strong-convexity

$$\underset{\mathbf{h}, \mathbf{v}}{\text{minimize}} \quad \sum_a \frac{\|\log \mathcal{L}_{a,.} - \log(a)\mathbf{h} - \mathbf{v}\|^2}{\text{Least-Squares}} + \lambda \frac{\mathcal{Q}(\mathbf{D}\mathbf{h}, \mathbf{D}\mathbf{v}; \alpha)}{\text{Total Variation}}$$

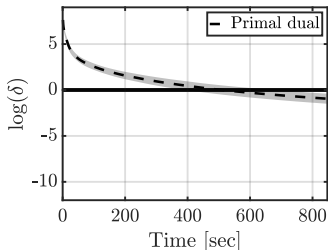


nonsmooth



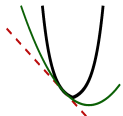
Primal-dual algorithm (Chambolle, 2011)

δ : duality gap, $\delta(\mathbf{x}^n, \mathbf{y}^n) \rightarrow 0$



Convexity properties

$$\underset{\mathbf{h}, \mathbf{v}}{\text{minimize}} \quad \sum_a \frac{\|\log \mathcal{L}_{a,.} - \log(a)\mathbf{h} - \mathbf{v}\|^2}{\text{Least-Squares}} + \lambda \frac{\mathcal{Q}(\mathbf{D}\mathbf{h}, \mathbf{D}\mathbf{v}; \alpha)}{\text{Total Variation}}$$



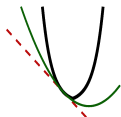
μ -strongly convex

nonsmooth



Convexity properties

$$\underset{\mathbf{h}, \mathbf{v}}{\text{minimize}} \quad \sum_a \frac{\|\log \mathcal{L}_{a,.} - \log(a)\mathbf{h} - \mathbf{v}\|^2}{\text{Least-Squares}} + \lambda \frac{\mathcal{Q}(\mathbf{D}\mathbf{h}, \mathbf{D}\mathbf{v}; \alpha)}{\text{Total Variation}}$$



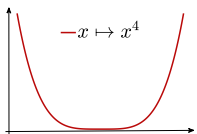
μ -strongly convex

nonsmooth

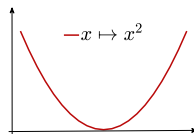


Strong-convexity

- φ μ -strongly convex iff $\varphi - \frac{\mu}{2} \|\cdot\|^2$ convex



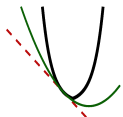
✓ strictly convex
✗ non strongly convex



✓ strictly convex
✓ 1-strongly convex

Convexity properties

$$\underset{\mathbf{h}, \mathbf{v}}{\text{minimize}} \quad \sum_a \frac{\|\log \mathcal{L}_{a,.} - \log(a)\mathbf{h} - \mathbf{v}\|^2}{\text{Least-Squares}} + \lambda \frac{\mathcal{Q}(\mathbf{D}\mathbf{h}, \mathbf{D}\mathbf{v}; \alpha)}{\text{Total Variation}}$$



μ -strongly convex

nonsmooth

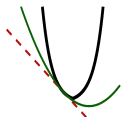


Strong-convexity

- φ μ -strongly convex iff $\varphi - \frac{\mu}{2} \|\cdot\|^2$ convex
- $\varphi \in \mathcal{C}^2$ with Hessian matrix $\mathbf{H}\varphi \succeq 0 \implies \mu = \min \text{Sp}(\mathbf{H}\varphi)$

Convexity properties

$$\underset{\mathbf{h}, \mathbf{v}}{\text{minimize}} \quad \sum_a \frac{\|\log \mathcal{L}_{a,.} - \log(a)\mathbf{h} - \mathbf{v}\|^2}{\text{Least-Squares}} + \lambda \frac{\mathcal{Q}(\mathbf{D}\mathbf{h}, \mathbf{D}\mathbf{v}; \alpha)}{\text{Total Variation}}$$



μ -strongly convex

nonsmooth



Strong-convexity

- φ μ -strongly convex iff $\varphi - \frac{\mu}{2} \|\cdot\|^2$ convex
- $\varphi \in \mathcal{C}^2$ with Hessian matrix $\mathbf{H}\varphi \succeq 0 \implies \mu = \min \text{Sp}(\mathbf{H}\varphi)$

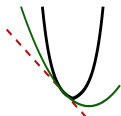
Proposition (Pascal, 2019)

$\sum_a \|\log \mathcal{L}_a - \log(a)\mathbf{h} - \mathbf{v}\|^2$ is μ -strongly convex.

$a_{\min} = 2^1, \quad a_{\max}$	2^2	2^3	2^4	2^5	2^6
$\mu = \min \text{Sp}(2\Phi^\top \Phi)$	0.29	0.72	1.20	1.69	2.20

Accelerated algorithm based on strong-convexity

$$\underset{\mathbf{h}, \mathbf{v}}{\text{minimize}} \quad \sum_a \frac{\|\log \mathcal{L}_{a,.} - \log(a) \mathbf{h} - \mathbf{v}\|^2}{\text{Least-Squares}} + \lambda \frac{\mathcal{Q}(\mathbf{D}\mathbf{h}, \mathbf{D}\mathbf{v}; \alpha)}{\text{Total Variation}}$$



μ -strongly convex

nonsmooth



Accelerated Primal-dual algorithm (*Chambolle, 2011*)

for $n = 0, 1, \dots$ $\mathbf{x} = (\mathbf{h}, \mathbf{v})$

$$\mathbf{y}^{n+1} = \text{prox}_{\sigma_n(\lambda\mathcal{Q})^*}(\mathbf{y}^n + \sigma_n \mathbf{D}\bar{\mathbf{x}}^n)$$

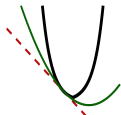
$$\mathbf{x}^{n+1} = \text{prox}_{\tau_n \|\mathcal{L} - \Phi \cdot\|_2^2} \left(\mathbf{x}^n - \tau_n \mathbf{D}^\top \mathbf{y}^{n+1} \right)$$

$$\theta_n = \sqrt{1 + 2\mu\tau_n}, \quad \tau_{n+1} = \tau_n / \theta_n, \quad \sigma_{n+1} = \theta_n \sigma_n$$

$$\bar{\mathbf{x}}^{n+1} = \mathbf{x}^{n+1} + \theta_n^{-1} (\mathbf{x}^{n+1} - \mathbf{x}^n)$$

Accelerated algorithm based on strong-convexity

$$\underset{\mathbf{h}, \mathbf{v}}{\text{minimize}} \quad \sum_a \frac{\|\log \mathcal{L}_{a,.} - \log(a)\mathbf{h} - \mathbf{v}\|^2}{\text{Least-Squares}} + \lambda \frac{\mathcal{Q}(\mathbf{D}\mathbf{h}, \mathbf{D}\mathbf{v}; \alpha)}{\text{Total Variation}}$$



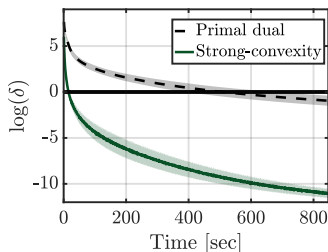
μ -strongly convex



nonsmooth

Accelerated Primal-dual algorithm (*Chambolle, 2011*)

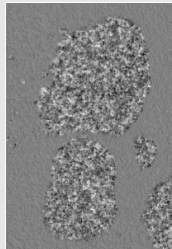
δ : duality gap, $\delta(\mathbf{x}^n, \mathbf{y}^n) \rightarrow 0$



Segmentation via iterated thresholding

$$\underset{\mathbf{h}, \mathbf{v}}{\text{minimize}} \quad \sum_a \frac{\|\log \mathcal{L}_{a,.} - \log(a)\mathbf{h} - \mathbf{v}\|^2}{\text{Least-Squares}} + \lambda \frac{\mathcal{Q}(\mathbf{D}\mathbf{h}, \mathbf{D}\mathbf{v}; \alpha)}{\text{Total Variation}}$$

Textured image



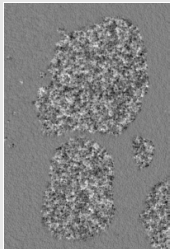
Lin. reg. $\hat{\mathbf{h}}^{\text{LR}}$



Segmentation via iterated thresholding

$$\underset{\mathbf{h}, \mathbf{v}}{\text{minimize}} \quad \sum_a \frac{\|\log \mathcal{L}_{a,.} - \log(a) \mathbf{h} - \mathbf{v}\|^2}{\text{Least-Squares}} + \lambda \frac{\mathcal{Q}(\mathbf{D}\mathbf{h}, \mathbf{D}\mathbf{v}; \alpha)}{\text{Total Variation}}$$

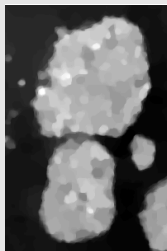
Textured image



Lin. reg. $\hat{\mathbf{h}}^{\text{LR}}$



Co-localized
contours $\hat{\mathbf{h}}^{\text{C}}$



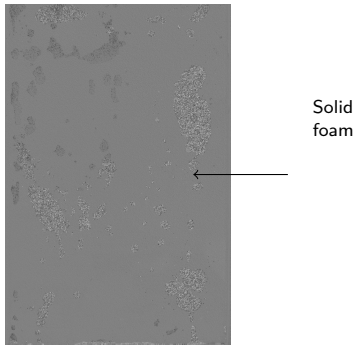
Threshold
estimate[†] $T\hat{\mathbf{h}}^{\text{C}}$



[†](Cai, 2013)

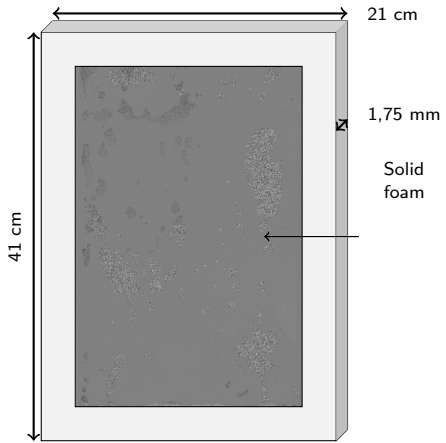
Multiphase flow through porous media

Laboratoire de Physique, ENS Lyon, V. Vidal, T. Busser, (M. Serres, IFPEN)



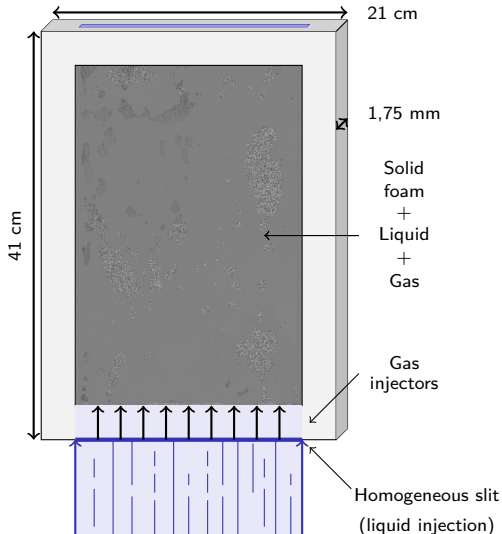
Multiphase flow through porous media

Laboratoire de Physique, ENS Lyon, V. Vidal, T. Busser, (M. Serres, IFPEN)



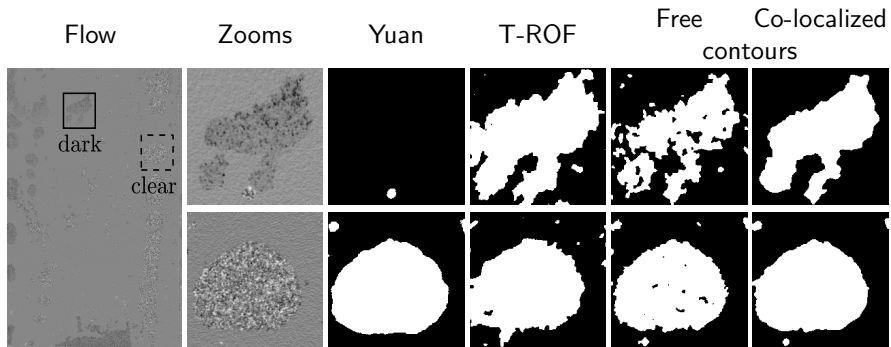
Multiphase flow through porous media

Laboratoire de Physique, ENS Lyon, V. Vidal, T. Busser, (M. Serres, IFPEN)

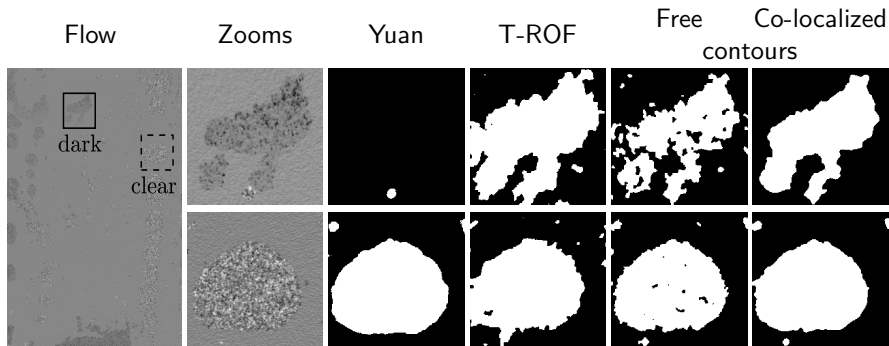


- 1600 × 1100 pixels
- video: ~ 1000 images
- phase diagram: ~ 10 flow rates

Low activity: $Q_G = 300\text{mL/min}$ - $Q_L = 300\text{mL/min}$



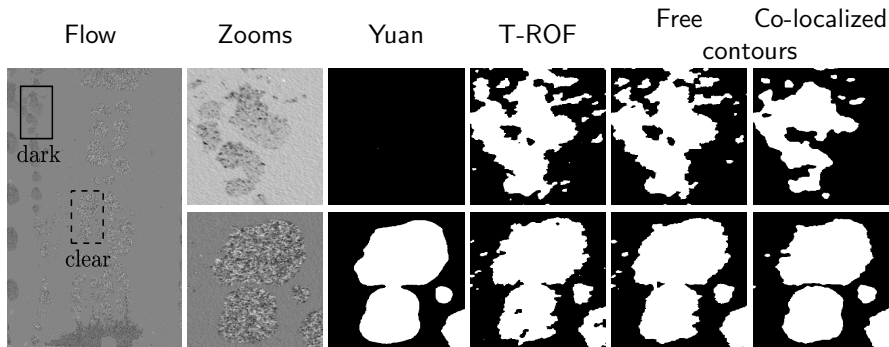
Low activity: $Q_G = 300\text{mL/min}$ - $Q_L = 300\text{mL/min}$



Liquid: $h_L = 0.4$ $\sigma_{\text{dark}}^2 = 10^{-2}$

Gas: $h_G = 0.9$ $\left| \begin{array}{l} \sigma_{\text{dark}}^2 = 10^{-2} \quad (\text{dark bubbles}) \\ \sigma_{\text{clear}}^2 = 10^{-1} \quad (\text{clear bubbles}) \end{array} \right.$

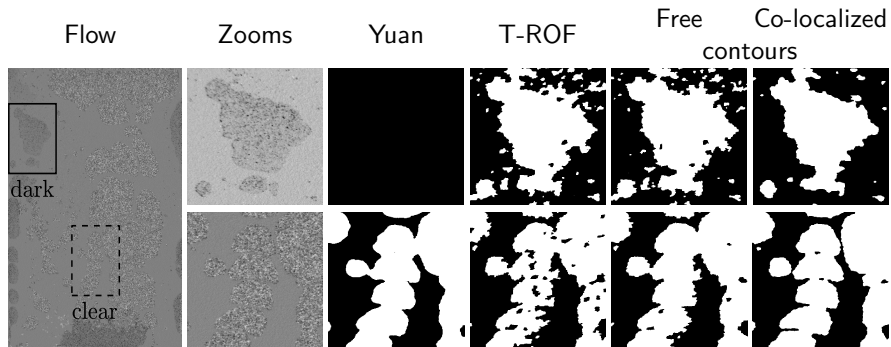
Transition: $Q_G = 400\text{mL/min}$ - $Q_L = 700\text{mL/min}$



Liquid: $h_L = 0.4$ $\sigma_{\text{dark}}^2 = 10^{-2}$

Gas: $h_G = 0.9$ $\left| \begin{array}{l} \sigma_{\text{dark}}^2 = 10^{-2} \quad (\text{dark bubbles}) \\ \sigma_{\text{clear}}^2 = 10^{-1} \quad (\text{clear bubbles}). \end{array} \right.$

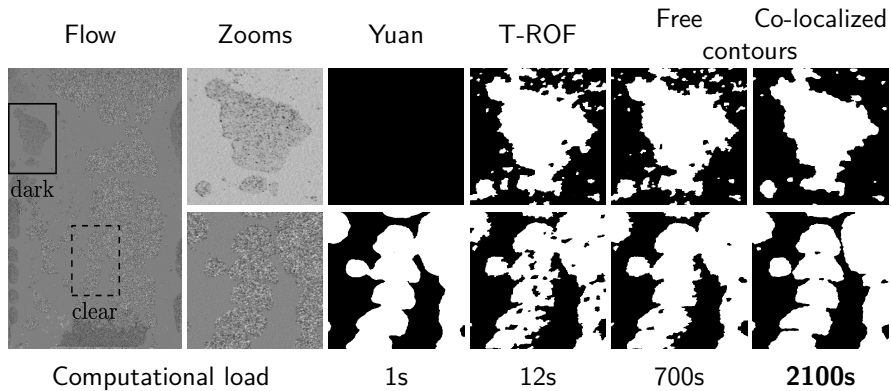
High activity: $Q_G = 1200\text{mL/min}$ - $Q_L = 300\text{mL/min}$



Liquid: $h_L = 0.4$ $\sigma_{\text{dark}}^2 = 10^{-2}$

Gas: $h_G = 0.9$ $\left| \begin{array}{l} \sigma_{\text{dark}}^2 = 10^{-2} \quad (\text{dark bubbles}) \\ \sigma_{\text{clear}}^2 = 10^{-1} \quad (\text{clear bubbles}). \end{array} \right.$

High activity: $Q_G = 1200\text{mL/min}$ - $Q_L = 300\text{mL/min}$



Liquid: $h_L = 0.4$ $\sigma_{\text{dark}}^2 = 10^{-2}$

Gas: $h_G = 0.9$ $\left| \begin{array}{l} \sigma_{\text{dark}}^2 = 10^{-2} \quad (\text{dark bubbles}) \\ \sigma_{\text{clear}}^2 = 10^{-1} \quad (\text{clear bubbles}). \end{array} \right.$

Regularization parameters selection

$$(\hat{\mathbf{h}}, \hat{\mathbf{v}}) (\mathcal{L}; \lambda, \alpha) = \operatorname{argmin}_{\mathbf{h}, \mathbf{v}} \sum_a \|\log \mathcal{L}_{a,.} - \log(a) \mathbf{h} - \mathbf{v}\|^2 + \lambda \mathcal{Q}(\mathbf{D}\mathbf{h}, \mathbf{D}\mathbf{v}; \alpha)$$

Regularization parameters selection

$$(\hat{\mathbf{h}}, \hat{\mathbf{v}}) (\mathcal{L}; \lambda, \alpha) = \operatorname{argmin}_{\mathbf{h}, \mathbf{v}} \sum_a \|\log \mathcal{L}_{a,.} - \log(a) \mathbf{h} - \mathbf{v}\|^2 + \lambda \mathcal{Q}(\mathbf{D}\mathbf{h}, \mathbf{D}\mathbf{v}; \alpha)$$

Lin. reg. $\hat{\mathbf{h}}^{\text{LR}}$

$$(\lambda, \alpha) = (0, 0)$$



Regularization parameters selection

$$(\hat{\mathbf{h}}, \hat{\mathbf{v}}) (\mathcal{L}; \lambda, \alpha) = \operatorname{argmin}_{\mathbf{h}, \mathbf{v}} \sum_a \|\log \mathcal{L}_{a,.} - \log(a) \mathbf{h} - \mathbf{v}\|^2 + \lambda \mathcal{Q}(\mathbf{D}\mathbf{h}, \mathbf{D}\mathbf{v}; \alpha)$$

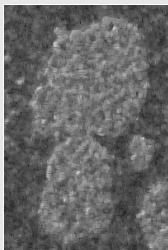
Lin. reg. $\hat{\mathbf{h}}^{\text{LR}}$

$$(\lambda, \alpha) = (0, 0)$$



Co-localized contours estimate $\hat{\mathbf{h}}^C$

$$(\lambda, \alpha) = (0.5, 0.5)$$



too small

Regularization parameters selection

$$(\hat{\mathbf{h}}, \hat{\mathbf{v}}) (\mathcal{L}; \lambda, \alpha) = \operatorname{argmin}_{\mathbf{h}, \mathbf{v}} \sum_a \|\log \mathcal{L}_{a,.} - \log(a) \mathbf{h} - \mathbf{v}\|^2 + \lambda \mathcal{Q}(\mathbf{D}\mathbf{h}, \mathbf{D}\mathbf{v}; \alpha)$$

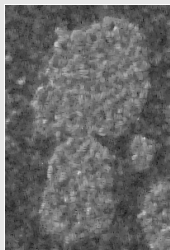
Lin. reg. $\hat{\mathbf{h}}^{\text{LR}}$

$$(\lambda, \alpha) = (0, 0)$$



Co-localized contours estimate $\hat{\mathbf{h}}^C$

$$(\lambda, \alpha) = (0.5, 0.5)$$



$$(\lambda, \alpha) = (500, 500)$$



too small

too large

Regularization parameters selection

$$(\hat{\mathbf{h}}, \hat{\mathbf{v}}) (\mathcal{L}; \lambda, \alpha) = \operatorname{argmin}_{\mathbf{h}, \mathbf{v}} \sum_a \|\log \mathcal{L}_{a,.} - \log(a) \mathbf{h} - \mathbf{v}\|^2 + \lambda \mathcal{Q}(\mathbf{D}\mathbf{h}, \mathbf{D}\mathbf{v}; \alpha)$$

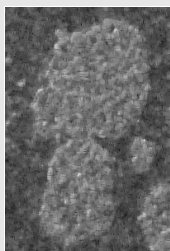
Lin. reg. $\hat{\mathbf{h}}^{\text{LR}}$

$$(\lambda, \alpha) = (0, 0)$$

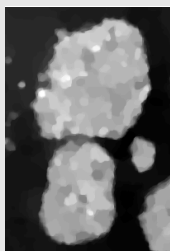


Co-localized contours estimate $\hat{\mathbf{h}}^C$

$$(\lambda, \alpha) = (0.5, 0.5)$$



$$(\lambda^\dagger, \alpha^\dagger) = (11.5, 0.8)$$



$$(\lambda, \alpha) = (500, 500)$$



too small

optimal

too large

What *optimal* means? How to determine λ^\dagger and α^\dagger ?

Parameter tuning (Grid search)

$$\left(\hat{\mathbf{h}}, \hat{\mathbf{v}} \right) (\mathcal{L}; \lambda, \alpha) = \underset{\mathbf{h}, \mathbf{v}}{\operatorname{argmin}} \sum_a \|\log \mathcal{L}_{a,.} - \log(a) \mathbf{h} - \mathbf{v}\|^2 + \lambda \mathcal{Q}(\mathbf{D}\mathbf{h}, \mathbf{D}\mathbf{v}; \alpha)$$

\mathbf{h} : discriminant, \mathbf{v} : auxiliary

Parameter tuning (Grid search)

$$\left(\hat{\mathbf{h}}, \hat{\mathbf{v}} \right) (\mathcal{L}; \lambda, \alpha) = \underset{\mathbf{h}, \mathbf{v}}{\operatorname{argmin}} \sum_a \| \log \mathcal{L}_{a,.} - \log(a) \mathbf{h} - \mathbf{v} \|^2 + \lambda \mathcal{Q}(\mathbf{D}\mathbf{h}, \mathbf{D}\mathbf{v}; \alpha)$$

\mathbf{h} : discriminant, \mathbf{v} : auxiliary

$\bar{\mathbf{h}}$: true regularity

$$\mathcal{R}(\lambda, \alpha) = \left\| \hat{\mathbf{h}}(\mathcal{L}; \lambda, \alpha) - \bar{\mathbf{h}} \right\|^2$$

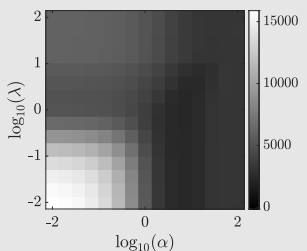
Parameter tuning (Grid search)

$$\left(\hat{\mathbf{h}}, \hat{\mathbf{v}} \right) (\mathcal{L}; \lambda, \alpha) = \underset{\mathbf{h}, \mathbf{v}}{\operatorname{argmin}} \sum_a \| \log \mathcal{L}_{a,.} - \log(a) \mathbf{h} - \mathbf{v} \|^2 + \lambda \mathcal{Q}(\mathbf{D}\mathbf{h}, \mathbf{D}\mathbf{v}; \alpha)$$

\mathbf{h} : discriminant, \mathbf{v} : auxiliary

$\bar{\mathbf{h}}$: true regularity

$$\mathcal{R}(\lambda, \alpha) = \left\| \hat{\mathbf{h}}(\mathcal{L}; \lambda, \alpha) - \bar{\mathbf{h}} \right\|^2$$



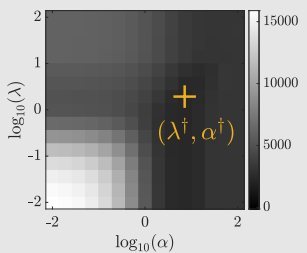
Parameter tuning (Grid search)

$$\left(\hat{\mathbf{h}}, \hat{\mathbf{v}} \right) (\mathcal{L}; \lambda, \alpha) = \underset{\mathbf{h}, \mathbf{v}}{\operatorname{argmin}} \sum_a \|\log \mathcal{L}_{a,.} - \log(a) \mathbf{h} - \mathbf{v}\|^2 + \lambda \mathcal{Q}(\mathbf{D}\mathbf{h}, \mathbf{D}\mathbf{v}; \alpha)$$

\mathbf{h} : discriminant, \mathbf{v} : auxiliary

$\bar{\mathbf{h}}$: true regularity

$$\mathcal{R}(\lambda, \alpha) = \left\| \hat{\mathbf{h}}(\mathcal{L}; \lambda, \alpha) - \bar{\mathbf{h}} \right\|^2$$



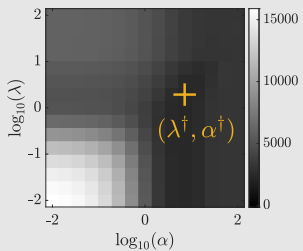
Parameter tuning (Grid search)

$$(\hat{\mathbf{h}}, \hat{\mathbf{v}}) (\mathcal{L}; \lambda, \alpha) = \underset{\mathbf{h}, \mathbf{v}}{\operatorname{argmin}} \sum_a \|\log \mathcal{L}_{a,.} - \log(a) \mathbf{h} - \mathbf{v}\|^2 + \lambda \mathcal{Q}(\mathbf{D}\mathbf{h}, \mathbf{D}\mathbf{v}; \alpha)$$

\mathbf{h} : discriminant, \mathbf{v} : auxiliary

$\bar{\mathbf{h}}$: true regularity

$$\mathcal{R}(\lambda, \alpha) = \left\| \hat{\mathbf{h}}(\mathcal{L}; \lambda, \alpha) - \bar{\mathbf{h}} \right\|^2$$



$\bar{\mathbf{h}}$: unknown!

?

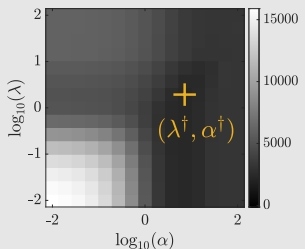
Parameter tuning (Grid search)

$$(\hat{\mathbf{h}}, \hat{\mathbf{v}}) (\mathcal{L}; \lambda, \alpha) = \underset{\mathbf{h}, \mathbf{v}}{\operatorname{argmin}} \sum_a \|\log \mathcal{L}_{a,.} - \log(a) \mathbf{h} - \mathbf{v}\|^2 + \lambda \mathcal{Q}(\mathbf{D}\mathbf{h}, \mathbf{D}\mathbf{v}; \alpha)$$

\mathbf{h} : discriminant, \mathbf{v} : auxiliary

$\bar{\mathbf{h}}$: true regularity

$$\mathcal{R}(\lambda, \alpha) = \left\| \hat{\mathbf{h}}(\mathcal{L}; \lambda, \alpha) - \bar{\mathbf{h}} \right\|^2$$



$\bar{\mathbf{h}}$: unknown!

?

Stein Unbiased Risk Estimate
(SURE)

Stein Unbiased Risk Estimate (Principle)

Observations $\mathbf{y} = \bar{\mathbf{x}} + \boldsymbol{\zeta} \in \mathbb{R}^P$, $\bar{\mathbf{x}}$: truth and $\boldsymbol{\zeta} \sim \mathcal{N}(\mathbf{0}, \rho^2 \mathbf{I})$

Stein Unbiased Risk Estimate (Principe)

Observations $\mathbf{y} = \bar{\mathbf{x}} + \boldsymbol{\zeta} \in \mathbb{R}^P$, $\bar{\mathbf{x}}$: truth and $\boldsymbol{\zeta} \sim \mathcal{N}(\mathbf{0}, \rho^2 \mathbf{I})$

Parametric estimator $(\mathbf{y}; \lambda) \mapsto \hat{\mathbf{x}}(\mathbf{y}; \lambda)$

Ex. $\hat{\mathbf{x}}(\mathbf{y}; \lambda) = \begin{cases} (\mathbf{I} + \lambda \mathbf{D}^\top \mathbf{D})^{-1} \mathbf{y} & \text{(linear)} \\ \underset{\mathbf{x}}{\operatorname{argmin}} \|\mathbf{y} - \mathbf{x}\|^2 + \lambda Q(\mathbf{Dx}) & \text{(nonlinear)} \end{cases}$

Stein Unbiased Risk Estimate (Principe)

Observations $\mathbf{y} = \bar{\mathbf{x}} + \boldsymbol{\zeta} \in \mathbb{R}^P$, $\bar{\mathbf{x}}$: truth and $\boldsymbol{\zeta} \sim \mathcal{N}(\mathbf{0}, \rho^2 \mathbf{I})$

Parametric estimator $(\mathbf{y}; \lambda) \mapsto \hat{\mathbf{x}}(\mathbf{y}; \lambda)$

Ex. $\hat{\mathbf{x}}(\mathbf{y}; \lambda) = \begin{cases} (\mathbf{I} + \lambda \mathbf{D}^\top \mathbf{D})^{-1} \mathbf{y} & \text{(linear)} \\ \underset{\mathbf{x}}{\operatorname{argmin}} \|\mathbf{y} - \mathbf{x}\|^2 + \lambda \mathcal{Q}(\mathbf{Dx}) & \text{(nonlinear)} \end{cases}$

Quadratic error $R(\lambda) \triangleq \mathbb{E}_{\boldsymbol{\zeta}} \|\hat{\mathbf{x}}(\mathbf{y}; \lambda) - \bar{\mathbf{x}}\|^2 \stackrel{?}{=} \mathbb{E}_{\boldsymbol{\zeta}} \widehat{R}(\mathbf{y}; \lambda)$ bar x unknown

Stein Unbiased Risk Estimate (Principe)

Observations $\mathbf{y} = \bar{\mathbf{x}} + \boldsymbol{\zeta} \in \mathbb{R}^P$, $\bar{\mathbf{x}}$: truth and $\boldsymbol{\zeta} \sim \mathcal{N}(\mathbf{0}, \rho^2 \mathbf{I})$

Parametric estimator $(\mathbf{y}; \lambda) \mapsto \hat{\mathbf{x}}(\mathbf{y}; \lambda)$

Ex. $\hat{\mathbf{x}}(\mathbf{y}; \lambda) = \begin{cases} (\mathbf{I} + \lambda \mathbf{D}^\top \mathbf{D})^{-1} \mathbf{y} & \text{(linear)} \\ \underset{\mathbf{x}}{\operatorname{argmin}} \|\mathbf{y} - \mathbf{x}\|^2 + \lambda Q(\mathbf{Dx}) & \text{(nonlinear)} \end{cases}$

Quadratic error $R(\lambda) \triangleq \mathbb{E}_{\boldsymbol{\zeta}} \|\hat{\mathbf{x}}(\mathbf{y}; \lambda) - \bar{\mathbf{x}}\|^2 \stackrel{?}{=} \mathbb{E}_{\boldsymbol{\zeta}} \widehat{R}(\mathbf{y}; \lambda)$ bar x unknown

Theorem (Stein, 1981)

Let $(\mathbf{y}; \lambda) \mapsto \hat{\mathbf{x}}(\mathbf{y}; \lambda)$ an estimator of $\bar{\mathbf{x}}$

- weakly differentiable w.r.t. \mathbf{y} ,
- such that $\boldsymbol{\zeta} \mapsto \langle \hat{\mathbf{x}}(\bar{\mathbf{x}} + \boldsymbol{\zeta}; \lambda), \boldsymbol{\zeta} \rangle$ is integrable w.r.t. $\mathcal{N}(\mathbf{0}, \rho^2 \mathbf{I})$.

$$\begin{aligned} \widehat{R}(\mathbf{y}; \lambda) &\triangleq \|\hat{\mathbf{x}}(\mathbf{y}; \lambda) - \mathbf{y}\|^2 + 2\rho^2 \operatorname{tr}(\partial_{\mathbf{y}} \hat{\mathbf{x}}(\mathbf{y}; \lambda)) - \rho^2 P \\ &\implies R(\lambda) = \mathbb{E}_{\boldsymbol{\zeta}} [\widehat{R}(\mathbf{y}; \lambda)]. \end{aligned}$$

Generalized Stein Unbiased Risk Estimate

Observations $\mathbf{y} = \Phi \bar{\mathbf{x}} + \zeta \in \mathbb{R}^P$, $\bar{\mathbf{x}} \in \mathbb{R}^N$, $\Phi : \mathbb{R}^{P \times N}$ and $\zeta \sim \mathcal{N}(\mathbf{0}, \mathcal{S})$

E.g. the estimators $\hat{\mathbf{h}}(\mathcal{L}; \lambda, \alpha)$ with free or co-localized contours

$$\log \mathcal{L} = \Phi(\bar{\mathbf{h}}, \bar{\mathbf{v}}) + \zeta \quad \zeta \sim \mathcal{N}(\mathbf{0}, \mathcal{S}) \quad \mathcal{R} = \|\hat{\mathbf{h}} - \bar{\mathbf{h}}\|^2$$

$$\Phi : (\mathbf{h}, \mathbf{v}) \mapsto \{\log(a)\mathbf{h} + \mathbf{v}\}_a \quad \begin{array}{|c|c|c|c|c|c|c|c|} \hline \cdot & \cdot & \cdot & \textcolor{darkgreen}{\cdot} & \cdot & \cdot & \cdot \\ \hline \cdot & \cdot & \cdot & \cdot & \cdot & \cdot & \cdot \\ \hline \end{array} \quad \Pi : (\mathbf{h}, \mathbf{v}) \mapsto (\mathbf{h}, \mathbf{0})$$

Projected estimation error $R_\Pi(\Lambda) \triangleq \mathbb{E}_\zeta \|\Pi \hat{\mathbf{x}}(\mathbf{y}; \Lambda) - \Pi \bar{\mathbf{x}}\|^2$

Generalized Stein Unbiased Risk Estimate

Observations $\mathbf{y} = \Phi \bar{\mathbf{x}} + \zeta \in \mathbb{R}^P$, $\bar{\mathbf{x}} \in \mathbb{R}^N$, $\Phi : \mathbb{R}^{P \times N}$ and $\zeta \sim \mathcal{N}(\mathbf{0}, \mathcal{S})$

E.g. the estimators $\hat{\mathbf{h}}(\mathcal{L}; \lambda, \alpha)$ with free or co-localized contours

$$\log \mathcal{L} = \Phi(\bar{\mathbf{h}}, \bar{\mathbf{v}}) + \zeta \quad \zeta \sim \mathcal{N}(\mathbf{0}, \mathcal{S}) \quad \mathcal{R} = \|\hat{\mathbf{h}} - \bar{\mathbf{h}}\|^2$$

$$\Phi : (\mathbf{h}, \mathbf{v}) \mapsto \{\log(a)\mathbf{h} + \mathbf{v}\}_a \quad \begin{array}{|c|c|c|c|c|c|c|c|c|c|c|} \hline & \cdot \\ \hline \cdot & \cdot \\ \hline \end{array} \quad \Pi : (\mathbf{h}, \mathbf{v}) \mapsto (\mathbf{h}, \mathbf{0})$$

Projected estimation error $R_{\Pi}(\Lambda) \triangleq \mathbb{E}_{\zeta} \|\Pi \hat{\mathbf{x}}(\mathbf{y}; \Lambda) - \Pi \bar{\mathbf{x}}\|^2$

Theorem (Pascal, 2020)

Let $(\mathbf{y}; \Lambda) \mapsto \hat{\mathbf{x}}(\mathbf{y}; \Lambda)$ an estimator of $\bar{\mathbf{x}}$

- weakly differentiable w.r.t. \mathbf{y} ,
- such that $\zeta \mapsto \langle \Pi \hat{\mathbf{x}}(\bar{\mathbf{x}} + \zeta; \lambda), \mathbf{A} \zeta \rangle$ is integrable w.r.t. $\mathcal{N}(\mathbf{0}, \mathcal{S})$.

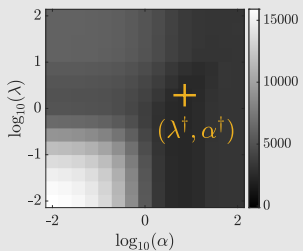
$$\begin{aligned} \hat{R}(\Lambda) &\triangleq \|\mathbf{A}(\Phi \hat{\mathbf{x}}(\mathbf{y}; \Lambda) - \mathbf{y})\|^2 + 2\text{tr} \left(\mathbf{S} \mathbf{A}^\top \Pi \partial_{\mathbf{y}} \hat{\mathbf{x}}(\mathbf{y}; \Lambda) \right) - \text{tr} \left(\mathbf{A} \mathbf{S} \mathbf{A}^\top \right) \\ &\implies R_{\Pi}(\Lambda) = \mathbb{E}_{\zeta} [\hat{R}(\Lambda)]. \end{aligned}$$

Parameter tuning (Grid search)

$$\left(\widehat{\boldsymbol{h}}, \widehat{\boldsymbol{v}}\right)(\mathcal{L}; \lambda, \alpha) = \operatorname{argmin}_{\boldsymbol{h}, \boldsymbol{v}} \sum_a \|\log \mathcal{L}_{a,.} - \log(a)\boldsymbol{h} - \boldsymbol{v}\|^2 + \lambda \mathcal{Q}(\mathbf{D}\boldsymbol{h}, \mathbf{D}\boldsymbol{v}; \alpha)$$

$\bar{\boldsymbol{h}}$: true regularity

$$\mathcal{R}(\lambda, \alpha) = \left\| \widehat{\boldsymbol{h}}(\mathcal{L}; \lambda, \alpha) - \bar{\boldsymbol{h}} \right\|^2$$



$\bar{\boldsymbol{h}}$: unknown!

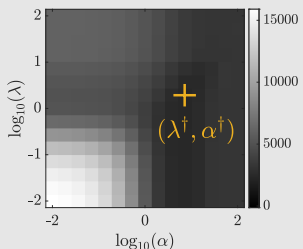
$$\widehat{R}_{\nu, \epsilon}(\mathcal{L}; \lambda, \alpha | \mathcal{S})$$

Parameter tuning (Grid search)

$$\left(\widehat{\boldsymbol{h}}, \widehat{\boldsymbol{v}}\right)(\mathcal{L}; \lambda, \alpha) = \operatorname{argmin}_{\boldsymbol{h}, \boldsymbol{v}} \sum_{\boldsymbol{a}} \|\log \mathcal{L}_{\boldsymbol{a}, \cdot} - \log(a)\boldsymbol{h} - \boldsymbol{v}\|^2 + \lambda \mathcal{Q}(\mathbf{D}\boldsymbol{h}, \mathbf{D}\boldsymbol{v}; \alpha)$$

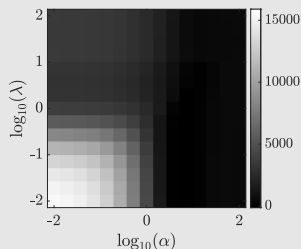
$\bar{\boldsymbol{h}}$: true regularity

$$\mathcal{R}(\lambda, \alpha) = \left\| \widehat{\boldsymbol{h}}(\mathcal{L}; \lambda, \alpha) - \bar{\boldsymbol{h}} \right\|^2$$



$\bar{\boldsymbol{h}}$: unknown!

$$\widehat{R}_{\nu, \epsilon}(\mathcal{L}; \lambda, \alpha | \mathcal{S})$$

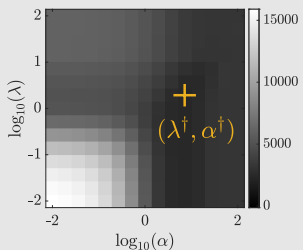


Parameter tuning (Grid search)

$$\left(\widehat{\boldsymbol{h}}, \widehat{\boldsymbol{v}}\right)(\mathcal{L}; \lambda, \alpha) = \operatorname{argmin}_{\boldsymbol{h}, \boldsymbol{v}} \sum_{\boldsymbol{a}} \|\log \mathcal{L}_{\boldsymbol{a}, \cdot} - \log(a)\boldsymbol{h} - \boldsymbol{v}\|^2 + \lambda \mathcal{Q}(\mathbf{D}\boldsymbol{h}, \mathbf{D}\boldsymbol{v}; \alpha)$$

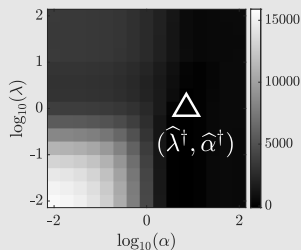
$\bar{\boldsymbol{h}}$: true regularity

$$\mathcal{R}(\lambda, \alpha) = \left\| \widehat{\boldsymbol{h}}(\mathcal{L}; \lambda, \alpha) - \bar{\boldsymbol{h}} \right\|^2$$



$\bar{\boldsymbol{h}}$: unknown!

$$\widehat{R}_{\nu, \varepsilon}(\mathcal{L}; \lambda, \alpha | \mathcal{S})$$

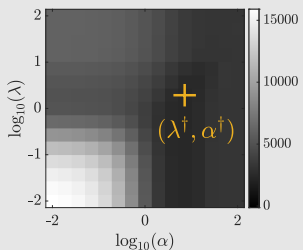


Parameter tuning (Grid search)

$$\left(\hat{\mathbf{h}}, \hat{\mathbf{v}}\right)(\mathcal{L}; \lambda, \alpha) = \operatorname{argmin}_{\mathbf{h}, \mathbf{v}} \sum_a \|\log \mathcal{L}_{a,.} - \log(a)\mathbf{h} - \mathbf{v}\|^2 + \lambda \mathcal{Q}(\mathbf{D}\mathbf{h}, \mathbf{D}\mathbf{v}; \alpha)$$

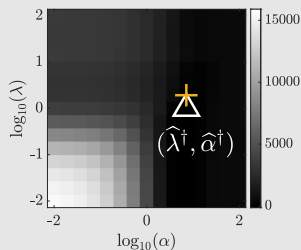
$\bar{\mathbf{h}}$: true regularity

$$\mathcal{R}(\lambda, \alpha) = \left\| \hat{\mathbf{h}}(\mathcal{L}; \lambda, \alpha) - \bar{\mathbf{h}} \right\|^2$$



$\bar{\mathbf{h}}$: unknown!

$$\hat{R}_{\nu, \varepsilon}(\mathcal{L}; \lambda, \alpha | \mathcal{S})$$

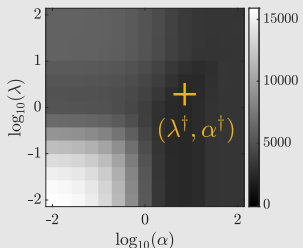


Parameter tuning (Automatic selection)

$$\left(\widehat{\boldsymbol{h}}, \widehat{\boldsymbol{v}}\right)(\mathcal{L}; \lambda, \alpha) = \operatorname{argmin}_{\boldsymbol{h}, \boldsymbol{v}} \sum_{\boldsymbol{a}} \|\log \mathcal{L}_{\boldsymbol{a}, \cdot} - \log(a)\boldsymbol{h} - \boldsymbol{v}\|^2 + \lambda \mathcal{Q}(\mathbf{D}\boldsymbol{h}, \mathbf{D}\boldsymbol{v}; \alpha)$$

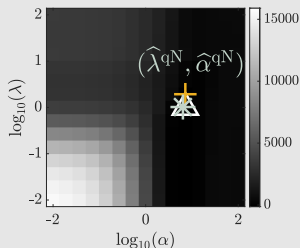
$\bar{\boldsymbol{h}}$: true regularity

$$\mathcal{R}(\lambda, \alpha) = \left\| \widehat{\boldsymbol{h}}(\mathcal{L}; \lambda, \alpha) - \bar{\boldsymbol{h}} \right\|^2$$



$\bar{\boldsymbol{h}}$: unknown!

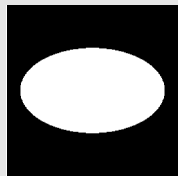
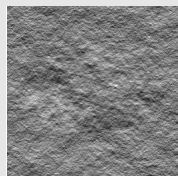
$$\widehat{R}_{\nu, \varepsilon}(\mathcal{L}; \lambda, \alpha | \mathcal{S})$$



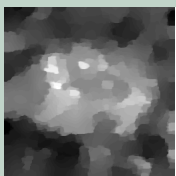
Automated selection of regularization parameters

$$(\hat{\mathbf{h}}, \hat{\mathbf{v}}) (\mathcal{L}; \lambda, \alpha) = \operatorname{argmin}_{\mathbf{h}, \mathbf{v}} \sum_a \|\log \mathcal{L}_{a,.} - \log(a) \mathbf{h} - \mathbf{v}\|^2 + \lambda \mathcal{Q}(\mathbf{D}\mathbf{h}, \mathbf{D}\mathbf{v}; \alpha)$$

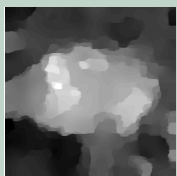
Example



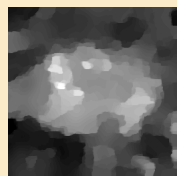
$\hat{\mathbf{h}}^F(\mathcal{L}; \lambda^\dagger, \alpha^\dagger)$
(grid)



$\hat{\mathbf{h}}^F(\mathcal{L}; \hat{\lambda}^\dagger, \hat{\alpha}^\dagger)$
(grid)



$\hat{\mathbf{h}}^F(\mathcal{L}; \hat{\lambda}^{qN}, \hat{\alpha}^{qN})$
(quasi-Newton)



225 calls of the estimator over the grid v.s. 40 for quasi-Newton

Part I: Fractal texture segmentation

Take home messages

- ▶ Fractal texture model based on local *regularity* and *variance*
 - * appropriate for real-world texture characterization
 - * complementary attributes able to finely discriminate

Take home messages

- ▶ Fractal texture model based on local *regularity* and *variance*
 - * appropriate for real-world texture characterization
 - * complementary attributes able to finely discriminate
- ▶ Simultaneous estimation and regularization
 - * significant decrease of the estimation error
 - * accurate and regular contours thanks to co-localized penalization

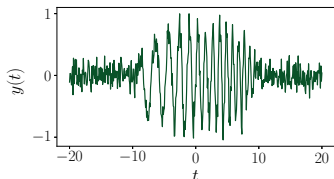
Take home messages

- ▶ Fractal texture model based on local *regularity* and *variance*
 - * appropriate for real-world texture characterization
 - * complementary attributes able to finely discriminate
- ▶ Simultaneous estimation and regularization
 - * significant decrease of the estimation error
 - * accurate and regular contours thanks to co-localized penalization
- ▶ Fast algorithms for automated tuning of hyperparameters
 - * possibility to manage huge amount of data
 - * amenable to process data corrupted by *correlated Gaussian noise*
 - * ensured objectivity and reproducibility

Part II: Point processes in time-frequency analysis

Time-frequency analysis of nonstationary signals

$y : \mathbb{R} \rightarrow \mathbb{C}$ function of time.



- electrical cardiac activity,
- audio recording,
- seismic activity,
- light intensity on a photosensor
- ...

Information of interest:

- time events e.g., an earthquake and its replica
- frequency content e.g., monitoring of the heart beating rate

time

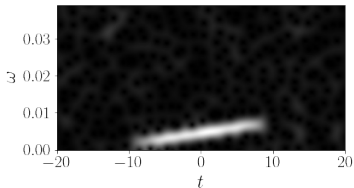
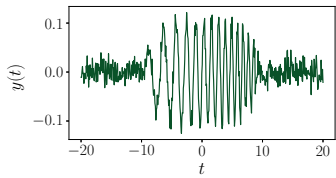
ever-changing world
marker of events and evolutions

frequency

waves, oscillations, rhythms
intrinsic mechanisms

Short-Time Fourier Transform with window h :

$$V_h y(t, \omega) \triangleq \int_{-\infty}^{\infty} \overline{y(u)} h(u - t) \exp(-i\omega u) du$$



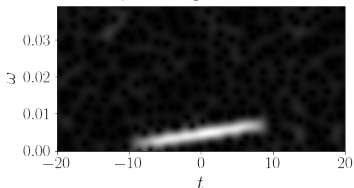
Energy density interpretation

$$\int \int_{-\infty}^{+\infty} |V_h y(t, \omega)|^2 dt \frac{d\omega}{2\pi} = \int_{-\infty}^{+\infty} |x(t)|^2 dt \quad \text{if} \quad \|h\|_2^2 = 1$$

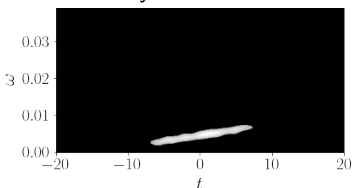
Signal, i.e., information of interest: regions of maximal energy.

Inversion formula $y(t) = \int \int_{-\infty}^{+\infty} \overline{V_h y(u, \omega)} h(t-u) \exp(i\omega u) du \frac{d\omega}{2\pi}$

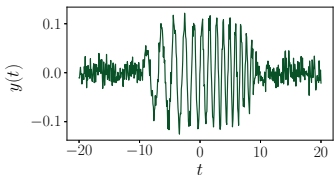
spectrogram



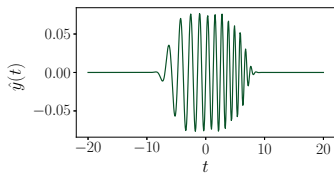
only maxima



noisy observation

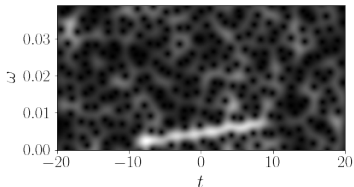


estimate

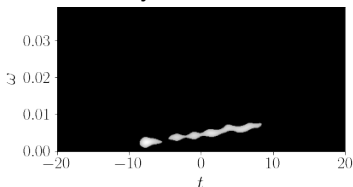


Inversion formula $y(t) = \int \int_{-\infty}^{+\infty} \overline{V_h y(u, \omega)} h(t-u) \exp(i\omega u) du \frac{d\omega}{2\pi}$

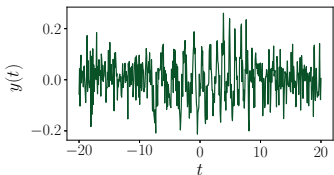
spectrogram



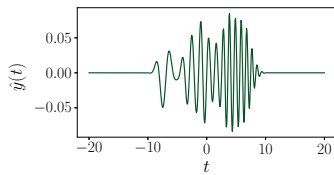
only maxima



noisy observation



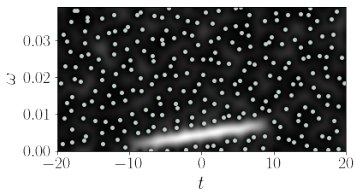
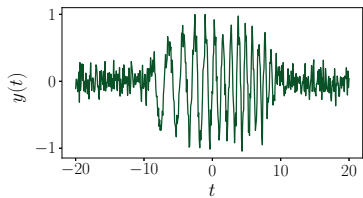
estimate



Maxima detection: reassignment, synchrosqueezing, ridge extraction

Restriction to the *circular Gaussian window*: $g(t) = \pi^{-1/4} e^{-t^2/2}$

Look for the zeros, i.e., the points (t_i, ω_i) such that $|V_g y(t_i, \omega_i)|^2 = 0$.

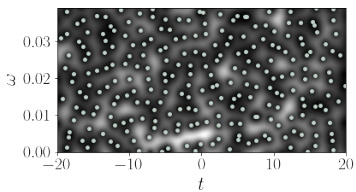
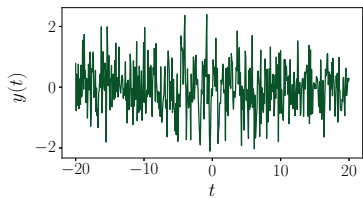


Observations: (Flandrin, 2015)

- In the noise region zeros are evenly spread.
- There exists a short-range repulsion between zeros.
- Zeros are repelled by the signal.

Restriction to the *circular Gaussian window*: $g(t) = \pi^{-1/4} e^{-t^2/2}$

Look for the zeros, i.e., the points (t_i, ω_i) such that $|V_g y(t_i, \omega_i)|^2 = 0$.

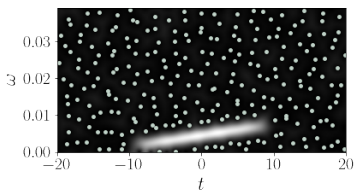
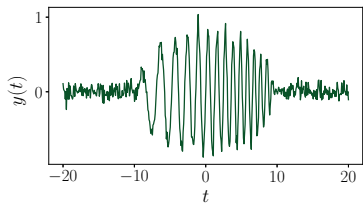


Observations: (Flandrin, 2015)

- In the noise region zeros are evenly spread.
- There exists a short-range repulsion between zeros.
- Zeros are repelled by the signal.

Restriction to the *circular Gaussian window*: $g(t) = \pi^{-1/4} e^{-t^2/2}$

Look for the zeros, i.e., the points (t_i, ω_i) such that $|V_g y(t_i, \omega_i)|^2 = 0$.

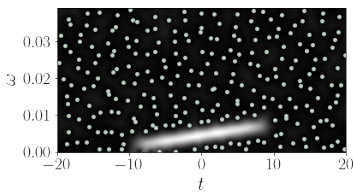
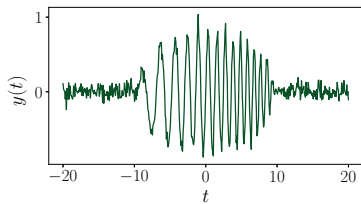


Observations: (Flandrin, 2015)

- In the noise region zeros are evenly spread.
- There exists a short-range repulsion between zeros.
- Zeros are repelled by the signal.

Restriction to the *circular Gaussian window*: $g(t) = \pi^{-1/4} e^{-t^2/2}$

Look for the zeros, i.e., the points (t_i, ω_i) such that $|V_g y(t_i, \omega_i)|^2 = 0$.



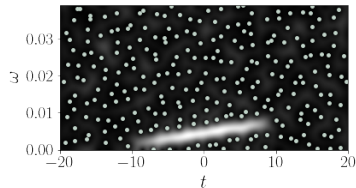
Observations: (Flandrin, 2015)

- In the noise region zeros are evenly spread.
- There exists a short-range repulsion between zeros.
- Zeros are repelled by the signal.

What can be said theoretically about the zeros of the spectrogram?

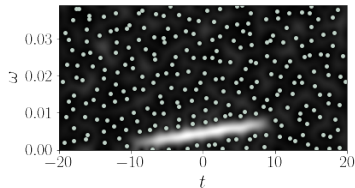
Unorthodox time-frequency analysis: spectrogram zeros

Idea assimilate the time-frequency plane with \mathbb{C} through $z = (\omega + it)/\sqrt{2}$



Unorthodox time-frequency analysis: spectrogram zeros

Idea assimilate the time-frequency plane with \mathbb{C} through $z = (\omega + it)/\sqrt{2}$



Bargmann factorization

$$V_g y(t, \omega) = e^{-|z|^2/2} e^{-i\omega t/2} B y(z)$$

Bargmann transform of the signal y

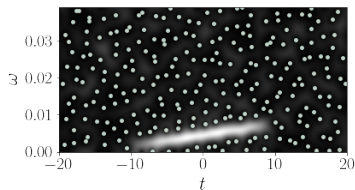
$$B y(z) \triangleq \pi^{-1/4} e^{-z^2/2} \int_{\mathbb{R}} \overline{y(u)} \exp \left(\sqrt{2} u z - u^2 / 2 \right) du,$$

$B y$ is an **entire** function, almost characterized by its infinitely many zeros:

$$B y(z) = z^m e^{C_0 + C_1 z + C_2 z^2} \prod_{n \in \mathbb{N}} \left(1 - \frac{z}{z_n} \right) \exp \left(\frac{z}{z_n} + \frac{1}{2} \left(\frac{z}{z_n} \right)^2 \right).$$

Unorthodox time-frequency analysis: spectrogram zeros

Idea assimilate the time-frequency plane with \mathbb{C} through $z = (\omega + it)/\sqrt{2}$



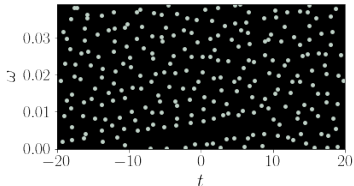
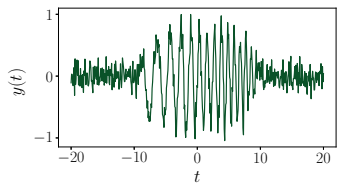
Bargmann factorization

$$V_g y(t, \omega) = e^{-|z|^2/2} e^{-i\omega t/2} B y(z)$$

Theorem The zeros of the Gaussian spectrogram $V_g y(t, \omega)$

- coincide with the zeros of the **entire** function $B y$,
- hence are **isolated** and constitute a **Point Process**,
- which almost completely **characterizes** the spectrogram.

(Flandrin, 2015)



Advantages of working with the zeros

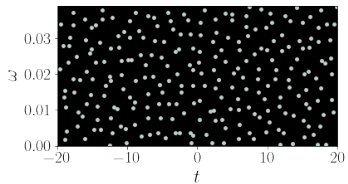
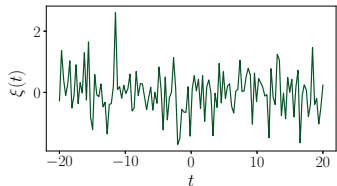
- Easy to find compared to relative maxima.
- Form a robust pattern in the time-frequency plane.
- Require little memory space for storage.
- Efficient tools were recently developed in **stochastic geometry**.

Need for a rigorous characterization of the distribution of the zeros.

The zeros of the spectrogram of white noise

Continuous complex white Gaussian noise

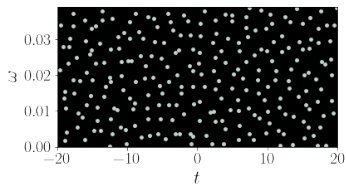
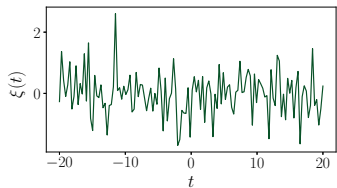
$$\xi(t) = \sum_{n=0}^{\infty} \xi[n] h_n(t), \quad \xi[n] \sim \mathcal{N}_{\mathbb{C}}(0, 1), \quad \{h_n, n = 0, 1, \dots\} \text{ Hermite functions}$$



The zeros of the spectrogram of white noise

Continuous complex white Gaussian noise

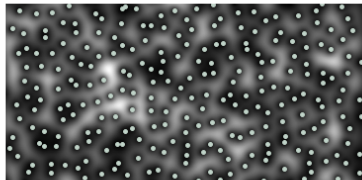
$$\xi(t) = \sum_{n=0}^{\infty} \xi[n] h_n(t), \quad \xi[n] \sim \mathcal{N}_{\mathbb{C}}(0, 1), \quad \{h_n, n = 0, 1, \dots\} \text{ Hermite functions}$$



Theorem $V_g \xi(t, \omega) = e^{-|z|^2/4} e^{-i\omega t/2} \text{GAF}_{\mathbb{C}}(z)$ (Bardenet & Hardy, 2021)

$\text{GAF}_{\mathbb{C}}(z) = \sum_{n=0}^{\infty} \xi[n] \frac{z^n}{\sqrt{n!}}$ is the *planar Gaussian Analytic Function*.

The zeros of the planar Gaussian Analytic Function



$$V_g \xi(t, \omega) \stackrel{\text{non-vanishing}}{\propto} \text{GAF}_{\mathbb{C}}(z)$$

$$z = (\omega + it)/\sqrt{2}$$

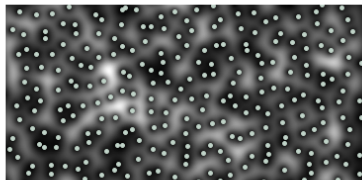
Zeros of $\text{GAF}_{\mathbb{C}}$: random set of points, i.e., a **Point Process**
characterized by a probability distribution on point configurations

Properties of the Point Process of the zeros of $\text{GAF}_{\mathbb{C}}$:

- invariant under the isometries of \mathbb{C} , i.e., **stationary**,
- has a uniform density $\rho^{(1)}(z) = \rho^{(1)} = 1/\pi$,
- explicit pair correlation function $\rho^{(2)}(z, z') = g_0(|z - z'|)$,
- scaling of the *hole probability*: $r^{-4} \log p_r \rightarrow -3e^2/4$, as $r \rightarrow \infty$

$$p_r = \mathbb{P}(\text{no point in the disk of center } 0 \text{ and radius } r)$$

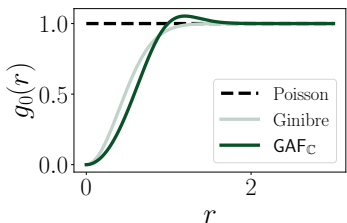
The zeros of the planar Gaussian Analytic Function



$$V_g \xi(t, \omega) \stackrel{\text{non-vanishing}}{\propto} \text{GAF}_{\mathbb{C}}(z)$$

$$z = (\omega + it)/\sqrt{2}$$

Zeros of $\text{GAF}_{\mathbb{C}}$: random set of points, i.e., a **Point Process**
characterized by a probability distribution on point configurations

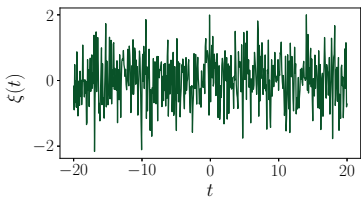


Pair correlation $\rho^{(2)}(z, z') dz dz' =$
 $\mathbb{P}(\text{1 point in } B(z, dz) \text{ and 1 in } B(z', dz'))$

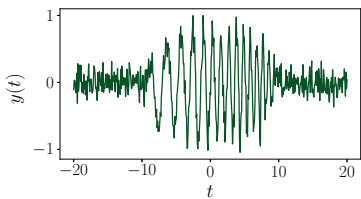
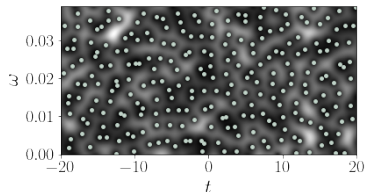
The point process of the zeros of the spectrogram is not **determinantal**.

Signal detection based on the spectrogram zeros

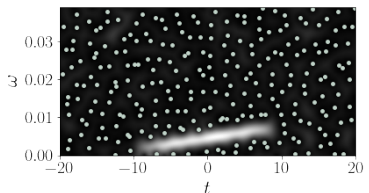
- H_0 white noisy only, i.e., $y(t) = \xi(t)$
- H_1 presence of a signal i.e., $y(t) = \text{snr} \times x(t) + \xi(t)$, $\text{snr} > 0$



null hypothesis

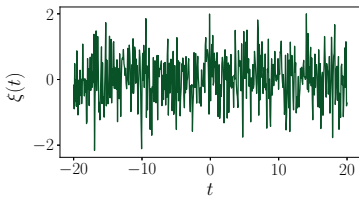


alternative hypothesis

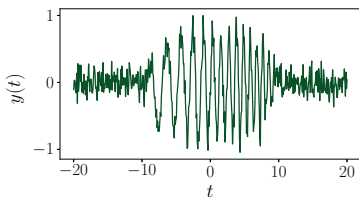
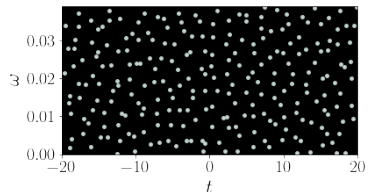


Signal detection based on the spectrogram zeros

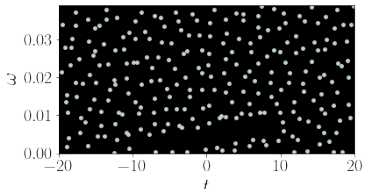
- H_0 white noisy only, i.e., $y(t) = \xi(t)$
- H_1 presence of a signal i.e., $y(t) = \text{snr} \times x(t) + \xi(t)$, $\text{snr} > 0$



null hypothesis



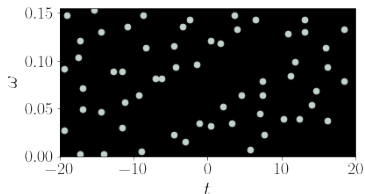
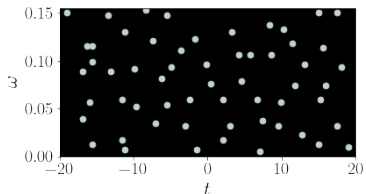
alternative hypothesis



Signal detection based on the spectrogram zeros

A functional statistic: the F -function

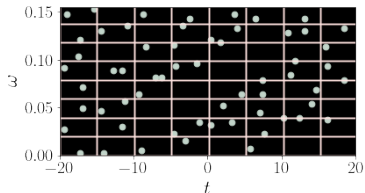
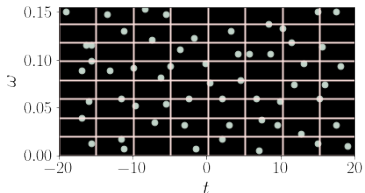
$$F(r) = \mathbb{P} \left(\inf_{z_i \in \mathcal{Z}} d(z_0, z_i) < r \right) : \text{empty space function}$$



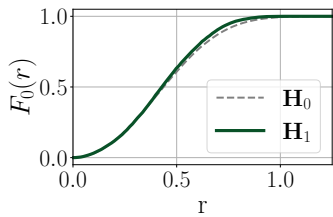
Signal detection based on the spectrogram zeros

A functional statistic: the F -function

$$F(r) = \mathbb{P} \left(\inf_{z_i \in \mathcal{Z}} d(z_0, z_i) < r \right) : \text{empty space function}$$



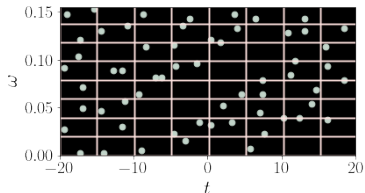
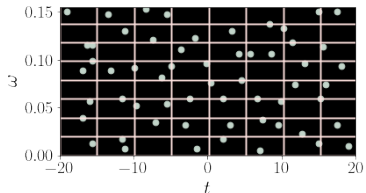
$$\hat{F}(r) = \frac{1}{N_{\#}} \sum_{j=1}^{N_{\#}} \mathbf{1} \left(\inf_{z \in \text{Zeros}} d(z_j, z) < r \right)$$



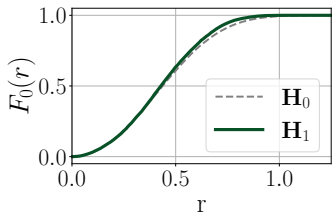
Signal detection based on the spectrogram zeros

A functional statistic: the F -function

$$F(r) = \mathbb{P} \left(\inf_{z_i \in \mathcal{Z}} d(z_0, z_i) < r \right) : \text{empty space function}$$

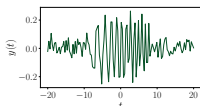


$$\hat{F}(r) = \frac{1}{N_{\#}} \sum_{j=1}^{N_{\#}} \mathbf{1} \left(\inf_{z \in \text{Zeros}} d(z_j, z) < r \right)$$

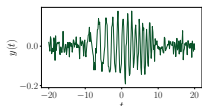


- Monte Carlo envelope test based on the discrepancy between \hat{F} and F_0

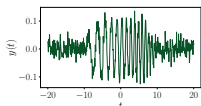
Signal detection based on the spectrogram zeros



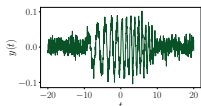
$N = 128$



$N = 256$

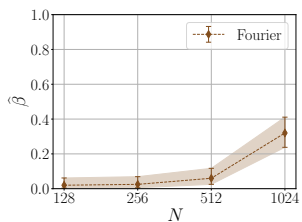


$N = 512$

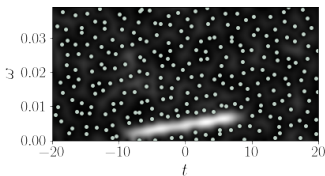


$N = 1024$

Performance: power of the test computed over 200 samples



- ✗ low detection power
- ✗ requires large number of samples

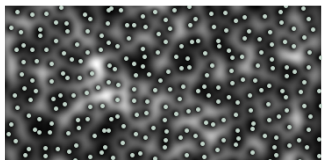


Limitations:

- necessary discretization of the STFT: arbitrary resolution
- observe only a bounded window: edge correction to compute $\widehat{F}(r)$

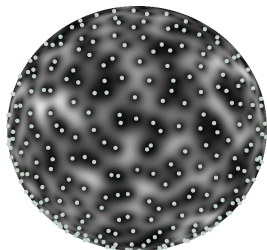
Short-Time Fourier Transform

$$V_g \xi(t, \omega) \propto \text{GAF}_{\mathbb{C}}(z) = \sum_{n=0}^{\infty} \xi[n] \frac{z^n}{\sqrt{n!}}$$



New transform?

$$? \propto \text{GAF}_{\mathbb{S}}(z) = \sum_{n=0}^N \xi[n] \sqrt{\binom{N}{n}} z^n$$



Time and frequency shifts

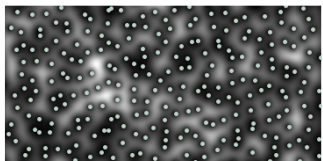
$$\mathbf{W}_{(t,\omega)}y(u) = e^{-i\omega u}y(u-t)$$

$$V_h[\mathbf{W}_{(t,\omega)}y](t', \omega') \stackrel{\text{covariance}}{=} e^{-i(\omega' - \omega)t} V_h y(t' - t, \omega' - \omega),$$

Coherent state interpretation

$$V_h y(t, \omega) = \langle y, \mathbf{W}_{(t,\omega)} h \rangle$$

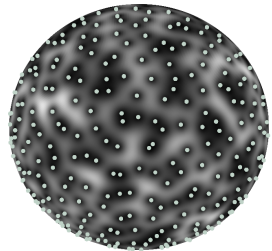
$\{\mathbf{W}_{(t,\omega)}h, t, \omega \in \mathbb{R}\}$ covariant family



Weyl-Heisenberg group $\{e^{i\gamma} \mathbf{W}_{(t,\omega)}, (\gamma, t, \omega) \in [0, 2\pi] \times \mathbb{R}^2\}$

$$\mathbf{W}_{(t', \omega')} \mathbf{W}_{(t, \omega)} = e^{i\omega t'} \mathbf{W}_{(t+t', \omega+\omega')}.$$

The Kravchuk transform: covariance under $\text{SO}(3)$

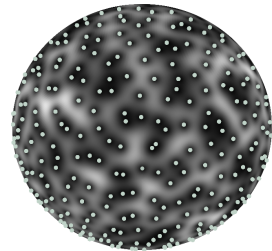


The Kravchuk transform: covariance under SO(3)

Coherent state interpretation $\mathbf{y} \in \mathbb{C}^{N+1}$

$$T\mathbf{y}(\vartheta, \varphi) = \langle \mathbf{y}, \Psi_{(\vartheta, \varphi)} \rangle$$

$$\vartheta \in [0, \pi], \varphi \in [0, 2\pi]$$

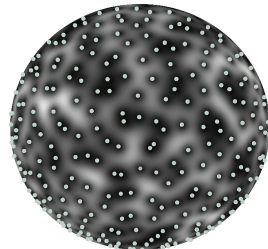


The Kravchuk transform: covariance under SO(3)

Coherent state interpretation $\mathbf{y} \in \mathbb{C}^{N+1}$

$$T\mathbf{y}(\vartheta, \varphi) = \langle \mathbf{y}, \Psi_{(\vartheta, \varphi)} \rangle$$

$$\vartheta \in [0, \pi], \varphi \in [0, 2\pi]$$



SO(3) **coherent states** (Gazeau, 2009)

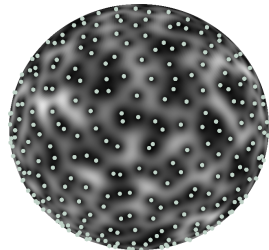
$$\Psi_{\vartheta, \varphi} = \sum_{n=0}^N \sqrt{\binom{N}{n}} \left(\cos \frac{\vartheta}{2} \right)^n \left(\sin \frac{\vartheta}{2} \right)^{N-n} e^{in\varphi} \mathbf{q}_n = \mathbf{R}_{\mathbf{u}(\vartheta, \varphi)} \Psi_{(0,0)},$$

The Kravchuk transform: covariance under SO(3)

Coherent state interpretation $\mathbf{y} \in \mathbb{C}^{N+1}$

$$T\mathbf{y}(\vartheta, \varphi) = \langle \mathbf{y}, \Psi_{(\vartheta, \varphi)} \rangle$$

$$\vartheta \in [0, \pi], \varphi \in [0, 2\pi]$$



SO(3) **coherent states** (Gazeau, 2009)

$$\Psi_{\vartheta, \varphi} = \sum_{n=0}^N \sqrt{\binom{N}{n}} \left(\cos \frac{\vartheta}{2} \right)^n \left(\sin \frac{\vartheta}{2} \right)^{N-n} e^{in\varphi} \mathbf{q}_n = \mathbf{R}_{\mathbf{u}(\vartheta, \varphi)} \Psi_{(0,0)},$$

Kravchuk transform

$\{\mathbf{q}_n, n = 0, 1, \dots, N\}$ the *Kravchuk functions*

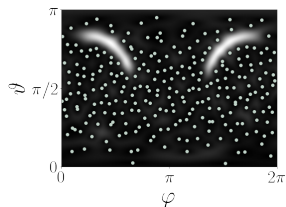
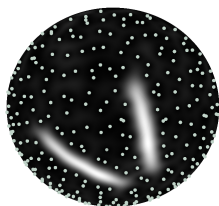
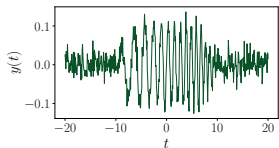
$$T\mathbf{y}(z) = \frac{1}{\sqrt{(1 + |z|^2)^N}} \sum_{n=0}^N \langle \mathbf{y}, \mathbf{q}_n \rangle \sqrt{\binom{N}{n}} z^n, \quad z = \cot(\vartheta/2) e^{i\varphi}$$

The Kravchuk transform: covariance under SO(3)

Kravchuk transform

$\{\mathbf{q}_n, n = 0, 1, \dots, N\}$ the *Kravchuk functions*

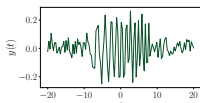
$$T\mathbf{y}(z) = \frac{1}{\sqrt{(1 + |z|^2)^N}} \sum_{n=0}^N \langle \mathbf{y}, \mathbf{q}_n \rangle \sqrt{\binom{N}{n}} z^n, \quad z = \cot(\vartheta/2) e^{i\varphi}$$



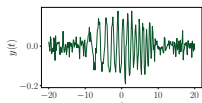
Contributions

- rigorous link: $T\xi(z) \stackrel{(\text{law})}{=} \sqrt{(1 + |z|^2)^{-N}} \text{GAF}_{\mathbb{S}}(z)$
- design of a robust implementation avoiding to compute $\langle \mathbf{y}, \mathbf{q}_n \rangle$
- spatial statistics on the sphere using the chordal distance: $\widehat{F}(r)$

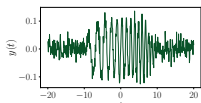
Signal detection based on the spectrogram zeros



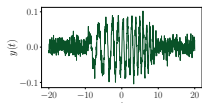
$N = 128$



$N = 256$

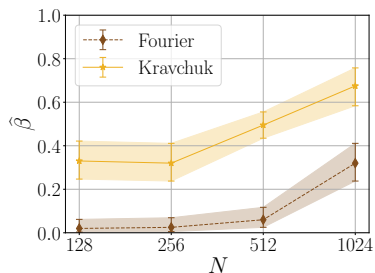


$N = 512$



$N = 1024$

Performance: power of the test computed over 200 samples



- ✓ higher detection power
- ✓ robust to small number of samples

- intrinsically encoded resolution: no need for prior knowledge
- compact phase space: no edge correction

Part II: Point Processes in time-frequency analysis

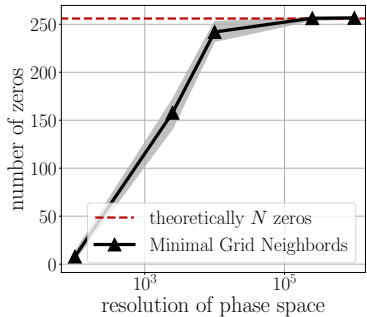
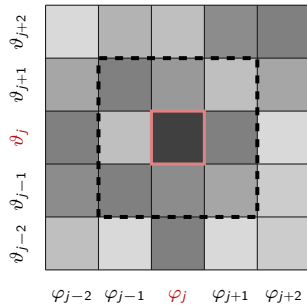
Take home messages

- ▶ a novel covariant discrete transform
 - * interpreted as a coherent state decomposition
 - * zeros of the Kravchuk spectrogram of white noise fully characterized
- ▶ signal processing based on spectrogram zeros
 - * preliminary work using the zeros of the Fourier spectrogram
 - * significant improvement using the Kravchuk spectrogram

Work in progress and perspectives

- ▶ convergence of the Kravchuk spectrogram toward the Fourier spectrogram
- ▶ interpretation of the action of $\text{SO}(3)$ on \mathbb{C}^{N+1}
- ▶ design of a FFT counterpart to compute the Kravchuk transform

Detection of the zeros of the Kravchuk spectrogram



Minimal Grid Neighbors

Purpose: summary statistic s , such that $\mathbb{E}[s(y)|\mathbf{H}_0] = 0$, $\mathbb{E}[s(y)|\mathbf{H}_1] > 0$

Test settings

- Level of significance α
- Number of samples under the null hypothesis m
- Index k , chosen so that $\alpha = k/(m + 1)$

Monte Carlo strategy

- (i) generate m independent samples of complex white Gaussian noise;
- (ii) compute their summary statistics $s_1 \geq s_2 \geq \dots \geq s_m$;
- (iii) compute the summary statistics of the observations \mathbf{y} under concern;
- (iv) if $s(\mathbf{y}) \geq s_k$, then reject the null hypothesis with confidence $1 - \alpha$.